NASA TECHNICAL NOTE

NASA TN D-5964

NASA TN D-5964

AN EQUATION FOR VORTEX MOTION
INCLUDING EFFECTS OF
BUOYANCY AND SOURCES WITH
APPLICATIONS TO TORNADOES

*by Robert C. Costen*

*Langley Research Center*
*Hampton, Va. 23365*

NATIONAL AERONAUTICS AND SPACE ADMINISTRATION • WASHINGTON, D. C. • OCTOBER 1970

0132824

| 1. Report No.<br>NASA TN D-5964 | 2. Government Accession No. | 3. |
|---|---|---|

| 4. Title and Subtitle<br>AN EQUATION FOR VORTEX MOTION INCLUDING EFFECTS OF BUOYANCY AND SOURCES WITH APPLICATIONS TO TORNADOES | 5. Report Date<br>October 1970 |
|---|---|
| | 6. Performing Organization Code |

| 7. Author(s)<br>Robert C. Costen | 8. Performing Organization Report No.<br>L-5738 |
|---|---|
| 9. Performing Organization Name and Address<br>NASA Langley Research Center<br>Hampton, Va. 23365 | 10. Work Unit No.<br>129-02-22-01 |
| | 11. Contract or Grant No. |
| 12. Sponsoring Agency Name and Address<br>National Aeronautics and Space Administration<br>Washington, D.C. 20546 | 13. Type of Report and Period Covered<br>Technical Note |
| | 14. Sponsoring Agency Code |

15. Supplementary Notes

16. Abstract

A new equation is derived for the motion of vorticity in a general fluid, including the effects of viscosity, compressibility, nonhomogeneity, and nonconservative forces. The equation holds, in particular, for vortices which may not move with the fluid. A linearized form of this equation is applied to tornado cyclones and to the twin tornado of April 11, 1965, near Elkhart, Indiana. It is shown that the displacement of tornado cyclones to the right of the mean tropospheric winds may be accounted for by the upward efflux of fluid from the cyclone into the jet stream. Also, the retarded revolution rate of the twin tornado may be due in part to an attractive "buoyancy" force acting on the partially rarefied cores of the pair.

| 17. Key Words (Suggested by Author(s))<br>Equation for vortex motion<br>Hydromagnetic vortex<br>Buoyant vortex<br>Source — vortex<br>Tornado<br>Cyclone | 18. Distribution Statement<br>Unclassified — Unlimited |
|---|---|

| 19. Security Classif. (of this report)<br>Unclassified | 20. Security Classif. (of this page)<br>Unclassified | 21. No. of Pages<br>66 | 22. Price*<br>$3.00 |
|---|---|---|---|

.

# CONTENTS

# AN EQUATION FOR VORTEX MOTION INCLUDING
# EFFECTS OF BUOYANCY AND SOURCES
# WITH APPLICATIONS TO TORNADOES

By Robert C. Costen
Langley Research Center

## SUMMARY

A new equation is derived for the motion of vorticity in a general fluid, including the effects of viscosity, compressibility, nonhomogeneity, and nonconservative forces. This equation results from a kinematical revision in the derivation of Kelvin's circulation theorem. It applies, in particular, to vortices which may not move with the fluid flow. The equation also admits fluid sources. The source term accounts for the influence of winds in one atmospheric layer on the motion of vortex tubes in an adjoining layer when a flux of fluid exists between the layers.

A linearized form of the equation is used to obtain possible explanations for (1) why tornado cyclones move to the right of the mean tropospheric winds, and (2) why the observed revolution rate of the funnels of a twin tornado about their common center was retarded with respect to the fluid flow. This twin tornado occurred on April 11, 1965, near Elkhart, Indiana.

It is shown that the rightward motion of tornado cyclones may be attributed on the basis of order-of-magnitude calculations to the upward flux of air from the core of the cyclone into the jet stream. It is also shown that a slowdown in the revolution rate of a twin tornado would result from (1) an attractive buoyancy force acting on each partially rarefied core in the presence of the radial pressure gradient of the other vortex or (2) an attractive magnetostatic force between axial dc electric currents of like sense in both cores. The retardation in revolution rate of the twin tornado due to buoyant attraction was estimated to be 5 percent. The electric current required for comparable retardation is on the order of $10^6$ amperes, which appears to be much too large for atmospheric phenomena. According to the linearized theory, the maximum possible retardation for two buoyant vortices of like circulations and cross sections is 22 percent. This figure applies to hollow vortices revolving about each other in near contact.

# INTRODUCTION

An accumulation of evidence exists that atmospheric vortices associated with severe storms do not necessarily move with the local fluid flow. According to reference 1, pp. 71-72, and reference 2, pp. 319-321, a storm cell which is destined to become severe moves with the mean tropospheric winds during the initial stages of formation. As the storm matures it acquires cyclonic rotation (being thereafter termed a tornado cylcone, see ref. 3, pp. 3-4) and commences to move at an angle of about $25^{\circ}$ to the right of the mean tropospheric winds in the northern hemisphere. This is an example of atmospheric vorticity which does not move with the fluid.

A second case of such deviate vortex motion is pointed up in this report. It concerns a twin tornado which occurred on April 11, 1965, near Elkhart, Indiana, and whose motion is documented in reference 4. Analysis of the data presented in this reference shows that the tornado pair apparently revolved about each other at a much slower rate than the fluid flow in which the tornadoes were immersed.

The explanation for these motions would seem to lie in a theory embracing the motion of vortex tubes, such as the circulation theorem of Kelvin (ref. 5, pp. 35-37). Kelvin obtained a formula for the time rate of change of vorticity flux $\dfrac{d}{dt} \iint \vec{\omega} \cdot \hat{n} \, dS$ through an arbitrary surface $S$ of finite area which moves with the fluid, where $\vec{\omega} = \text{curl } \vec{v}$ is vorticity and $\hat{n}$ is the unit normal on $S$. (See ref. 5, pp. 35-37, and ref. 6, pp. 150-151, 162. By Stokes' theorem $\dfrac{d}{dt} \iint \vec{\omega} \cdot \hat{n} \, dS = \dfrac{d}{dt} \oint \vec{v} \cdot \vec{dl}$ which is the time rate of change of circulation about the closed circuit line $l$ which bounds surface $S$ and moves with the fluid.) When the fluid is inviscid and subjected to conservative forces only, and when the density is either a constant or a single-valued function of the pressure (autobarotropic fluid), this formula reduces to $\dfrac{d}{dt} \iint \vec{\omega} \cdot \hat{n} \, dS = 0$, from which the conclusion is reached that under these conditions, the vorticity moves with the fluid. The expression $\dfrac{d}{dt} \iint \vec{\omega} \cdot \hat{n} \, dS$ was also considered by Helmholtz, V. Bjerknes, and others (as mentioned in refs. 7 and 8). V. Bjerknes evaluated the expression for the case of an inviscid nonbarotropic fluid and considered the effect of the Coriolis force (as discussed in ref. 9, pp. 233-261). The expression for $\dfrac{d}{dt} \iint \vec{\omega} \cdot \hat{n} \, dS$ in a viscous, compressible fluid is given in reference 10, pp. 51-52.

But in all these treatments the surface of integration $S$ (or bounding circuit loop $l$) is taken to move with the fluid. What is desired is to have $S$ and $l$ move with the vorticity, independent of the fluid, when these two motions are not the same. This distinction, being purely kinematical, is readily incorporated. The purpose of this report

is to modify the previous formulas for $\dfrac{d}{dt} \iint \vec{\omega} \cdot \hat{n} \, dS$ for application in the general case where surfaces of integration S may move in a manner different from that of the fluid, and to derive therefrom an unrestricted formula for the motion of the vortex tubes in a general fluid. A linearized form of this formula is then applied in rudimentary attempts to account for the two cases of atmospheric vortex motions cited. The formula may also apply to the motions of hurricanes and frontal cyclones, although these cases are not treated herein. A different approach to the movement of rotating storms is presented in reference 11.

All the usual terms of meteorological importance, such as the viscous terms and the Coriolis and centrifugal forces, are included in deriving the equation for vortex motion. In addition to these terms, fluid sources are included as a simple means of considering the influence of winds in one atmospheric layer on the motion of vortices in an adjoining layer when a flux of fluid exists between the layers.

The derivation of the magnetic and velocity fields at the ground plane near a tilted hydromagnetic vortex is given in appendix A. Appendix B is a description and tabulation of empirical data on the twin tornado of April 11, 1965, near Elkhart, Indiana. In appendix C the circulation of the twin tornado is deduced from its revolution rate.

## SYMBOLS AND NOTATION

A          cross-sectional area of vortex tube, $m^2$

a          radius of funnel A of twin tornado J-2 at ground, m

b          ratio of circulations, $\Gamma_B/\Gamma_A$

c          dimensionless parameter (eq. (42))

$D \equiv \sqrt{1 - \sin^2\chi \, \cos^2\psi_A} \, \sqrt{1 + \tan^2\chi \, \sin^2\psi_A}$  (see eq. (70c))

$\vec{E}$          electric field, V/m

$\vec{F}$          Lorentz force per unit length, N/m

$\vec{f}$          Lorentz force per unit volume, $N/m^3$

$G = \dfrac{\Gamma}{2\pi}$

$\vec{H}$      magnetic field, A/m

$\vec{I}$      axial electric current (figs. 11 and 12), A

$i$      effective axial electric current (eqs. (71b) and (71d)), A

$\vec{J}$      electric current density, $A/m^2$

$K = \dfrac{Q^*}{2\pi}$

$L$      length, m

$l$      circuit line of integration, m

$M$      excess mass present in a vortex tube per unit length, kg/m

$\hat{n}$      unit normal

$P$      center point of revolution of twin tornado J-2 at the ground (figs. 11 and 19)

$\overline{\overline{p}}$      pressure tensor including viscous terms, $N/m^2$

$p$      scalar pressure, $N/m^2$

$p'(\rho)$      pressure field which is single-valued function of density (eq. (23)), $N/m^2$

$p''$      deviation of pressure from single-valued function of density, (eq. (23)), $N/m^2$

$\mathcal{Q}$      total fluid source strength, kg/sec

$Q$      mass of source fluid being added to a vortex tube per unit length per unit time (eq. (36)), kg/m-sec

$Q^*$      fictitious source (sink) strength per unit length in a vortex tube having convergent flow and updraft, kg/m-sec (see section entitled "Tornado model")

$Q_e$      electric charge, C

$q$      source density; mass per unit volume and per unit time being added to a flow from a fluid source, $kg/m^3$-sec

4

| | |
|---|---|
| R | radius from tornado touchdown point in ground plane, m |
| $R_c$ | center-to-center distance between touchdown spots of funnels A and B of twin tornado J-2, m |
| $r_A$ | distance of vortex  A  from center point of revolution  P  of twin vortices in ground plane (figs. 11 and 19), m |
| $r_B$ | distance of vortex  B  from center point of revolution  P  of twin vortices in ground plane (figs. 11 and 19), m |
| S | surface area of integration, $m^2$ |
| t | time, sec |
| $\vec{U}$ | velocity of displacement of vorticity, m/sec |
| $\vec{U}'$ | arbitrary abstract velocity field utilized to describe the motion of regions of integration  S  and  V, m/sec |
| V | volume of integration, $m^3$ |
| $\vec{v}$ | fluid velocity field, m/sec |
| x,y,z | Cartesian coordinates, m |
| $\alpha$ | angle shown in figure 16, rad |
| $\beta$ | dimensionless parameter (eq. (62c)) |
| $\Gamma$ | circulation of a fluid vortex, $m^2$/sec |
| $\gamma$ | effective circulation of a fluid vortex (eqs. (70b) and (70e)), $m^2$/sec |
| $\epsilon$ | small dimensionless parameter |
| $\epsilon_0$ | permittivity of vacuum, F/m |
| $\theta$ | angle depicted in figures 13, 14, and 15, rad |

$\kappa$   ratio of axial electric current to circulation for a hydromagnetic vortex (eq. (83)), A-sec/m$^2$

$\Lambda$   dimensionless parameter (eq. (61))

$\lambda,\mu,\nu$   direction cosines

$\mu_o$   permeability of vacuum, H/m

$\xi,\eta,\zeta$   Cartesian coordinates used in figures 13 and 14

$\rho$   mass density, kg/m$^3$

$\rho'(p)$   density field which is a single-valued function of pressure (eq. (19)), kg/m$^3$

$\rho''$   deviation of density field from single-valued function of pressure (eq. (19)), kg/m$^3$

$\rho_e$   electric-charge density, C/m$^3$

$\vec{\tau}$   vector shown in figure 16

$\Phi$   gravitational potential (including centrifugal force in the rotating frame of the earth), J/kg

$\phi$   arbitrary scalar function, m$^2$/sec$^2$

$\varphi$   azimuth angle in symmetrical coordinate system of figure 13, rad

$\chi$   tilt angle of vortex with respect to the vertical (figs. 4 and 8), rad

$\psi$   azimuth angle in ground plane of figures 15 to 18, rad

$\psi_A, \psi_B$   azimuth angles shown in figures 11 and 19, rad

$\dot{\psi}_A(I)$   retarded revolution rate of twin vortices with axial electric current I, rad/sec

$\vec{\Omega}$   angular velocity of rotation of the earth, rad/sec

6

$\vec{\omega}$          fluid vorticity, curl $\vec{v}$, sec$^{-1}$

Superscripts:

A          funnel A of twin tornado J-2 (fig. 4)

B          funnel B of twin tornado J-2 (fig. 4)

bl          boundary layer at ground

js          jet stream

o          unperturbed vector fields in perturbation expansion

s          source fluid

1          first-order vector fields in perturbation expansion

Subscripts:

A          funnel A of twin tornado J-2 (fig. 4)

B          funnel B of twin tornado J-2 (fig. 4)

m          moving point

o          unperturbed scalar fields in perturbation expansion

$R, \varphi$          components in spherical coordinate system $R, \varphi, \theta$ (figs. 13 and 14)

$R, \psi, z$          components in cylindrical coordinate system (figs. 15 to 18)

x,y,z          Cartesian components of a vector

$\zeta$          component in Cartesian coordinate system $\xi, \eta, \zeta$ (figs. 13 and 14)

1          first-order scalar fields in perturbation expansion

$\perp$          field component perpendicular to the ground or to the lower jet-stream boundary

Mathematical notation:

$\rightarrow$          vector (arrow is omitted for magnitude of a vector)

$\langle\ \rangle$          mean value over a time interval or space interval

$\char`^$          unit vector

Dots over a symbol denote time derivatives.

Designations:

A          funnel A of twin tornado J-2; touchdown point of funnel A

B          funnel B of twin tornado J-2; touchdown point of funnel B

J-2          twin tornado of April 11, 1965, near Elkhart, Indiana

## DERIVATION OF GENERAL EQUATION FOR
## MOTION OF VORTICITY

### Fluid Sources

Conservation-of-mass equation with fluid sources in integral form.- The condensation of water vapor in the atmosphere into rain or hail, which subsequently falls to the earth, is an example of naturally occurring sink flow (or negative source flow). The conservation-of-mass equation for the main fluid excluding the rain or hail is, in integral form (ref. 6, pp. 132-133),

$$\iiint \frac{\partial \rho}{\partial t}\, dV + \oiint \rho \vec{v} \cdot \hat{n}\, dS = \iiint q\, dV \tag{1}$$

where the integrals extend over an arbitrary spatial volume V and its bounding surface S, with $\hat{n}$ taken as the outward unit normal on S. In this equation $\rho$ is the density of air and water vapor comprising the flow under consideration, $\vec{v}$ is its velocity field, and q is the rate at which mass density is being added to this flow from the source. (The source term q is negative for condensation, and positive for evaporation or sublimation.)

Conservation-of-momentum equation with fluid sources in integral form.- If the rain or hail, which will be termed the source fluid, may be described by a velocity field $\vec{v}^S$,

8

which is distinct from $\vec{v}$, then momentum is also transferred from the source fluid to the main flow at the rate of $q\vec{v}^S$ per unit volume. The conservation-of-momentum equation for the main flow becomes, in integral form (ref. 6, pp. 132-138, and ref. 9, pp. 233-236),

$$\iiint \frac{\partial}{\partial t}(\rho\vec{v})dV + \oiint\left[\rho\vec{v}(\vec{v}\cdot\hat{n}) - \overleftrightarrow{p}\cdot\hat{n}\right]dS = \iiint\left[q\vec{v}^S + \rho\left(\text{grad }\Phi + 2\vec{v}\times\vec{\Omega}\right) + \vec{f}\right]dV \tag{2}$$

where

$\overleftrightarrow{p}$          pressure tensor (including viscous terms), $N/m^2$

$\Phi$          gravitational potential (including centrifugal force in the rotating frame of the earth), J/kg

$2\rho\left(\vec{v}\times\vec{\Omega}\right)$    Coriolis force density, $N/m^3$

$\vec{\Omega}$          angular velocity of the earth, rad/sec

$\vec{f}$          Lorentz force density, $\rho_e\vec{E} + \mu_o\vec{J}\times\vec{H}$, $N/m^3$

      In equation (2) the first integral represents the time rate of increase of momentum contained in spatial volume V, the second integral is the rate of efflux of momentum through the closed bounding surface S by convection and by the action of the surface tractions, and the third integral gives the rate at which momentum is being added to volume V by transfer from the source fluid, and by the action of the gravitational, Coriolis, and Lorentz forces.

Conservation equations in differential form.- In differential form equation (1) is

$$\frac{\partial\rho}{\partial t} + \text{div }\rho\vec{v} = q \tag{3}$$

and equation (2) is

$$\rho\frac{\partial\vec{v}}{\partial t} + \vec{v}\frac{\partial\rho}{\partial t} + \vec{v}\text{ div }\rho\vec{v} + \rho\text{ grad }\frac{v^2}{2} - \rho\left(\vec{v}\times\vec{\omega}\right) - \text{div }\overleftrightarrow{p} = q\vec{v}^S + \rho\text{ grad }\Phi + 2\rho\vec{v}\times\vec{\Omega} + \vec{f} \tag{4}$$

where $v^2 = \vec{v}\cdot\vec{v}$ and $\vec{\omega} = \text{curl }\vec{v}$ (vorticity). When combined and divided by $\rho$, as is customarily done, these two equations give

$$\frac{\partial\vec{v}}{\partial t} - \vec{v}\times\vec{\omega} + \text{grad }\frac{v^2}{2} - \frac{1}{\rho}\text{div }\overleftrightarrow{p} + \frac{q}{\rho}\left(\vec{v} - \vec{v}^S\right) - \text{grad }\Phi - 2\vec{v}\times\vec{\Omega} - \frac{\vec{f}}{\rho} = 0 \tag{5a}$$

9

which for Cartesian coordinates may also be written

$$\left(\frac{\partial}{\partial t} + \vec{v} \cdot \text{grad}\right)\vec{v} = \frac{1}{\rho} \text{div} \, \overleftrightarrow{p} - \frac{q}{\rho}\left(\vec{v} - \vec{v}^S\right) + \text{grad} \, \Phi + 2\vec{v} \times \vec{\Omega} + \frac{\vec{f}}{\rho} \tag{5b}$$

## Vorticity Equation

The vorticity equation is obtained by taking the curl of equation (5a)

$$\frac{\partial \vec{\omega}}{\partial t} + \text{curl}\left[-\left(\vec{v} \times \vec{\omega}\right) - \frac{1}{\rho} \text{div} \, \overleftrightarrow{p} + \frac{q}{\rho}\left(\vec{v} - \vec{v}^S\right) - 2\vec{v} \times \vec{\Omega} - \frac{\vec{f}}{\rho}\right] = 0 \tag{6}$$

An integral form of this equation is given by

$$\iint \frac{\partial \vec{\omega}}{\partial t} \cdot \hat{n} \, dS + \iint \hat{n} \cdot \text{curl}\left[-\left(\vec{v} \times \vec{\omega}\right) - \frac{1}{\rho} \text{div} \, \overleftrightarrow{p} + \frac{q}{\rho}\left(\vec{v} - \vec{v}^S\right) - 2\vec{v} \times \vec{\Omega} - \frac{\vec{f}}{\rho}\right]dS = 0 \tag{7}$$

where the integrals are taken over an arbitrary spatial surface $S$ of finite area, and $\hat{n}$ is the unit normal on $S$, as shown in figure 1.
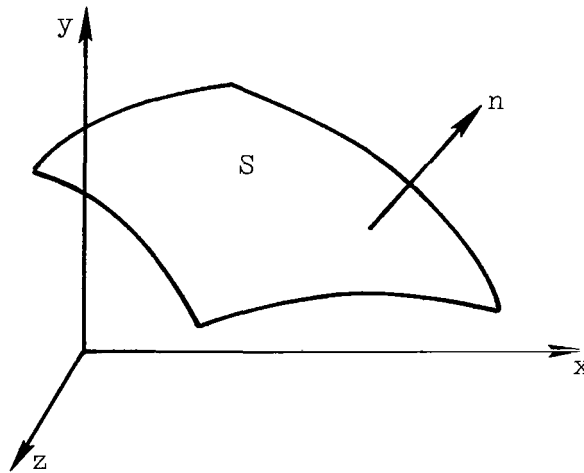


Figure 1.- Arbitrary surface $S$ with unit normal $\hat{n}$.

## Kinematics

Since the integrals in equation (7) are taken with time $t$ fixed, the surface of integration $S$ may be regarded as moving and deforming in an arbitrary continuous manner. Not being a material surface, $S$ need not move with the velocity $\vec{v}$ of the fluid medium. Instead, imagine surface $S$ to be moving and deforming in accordance with some arbitrary abstract velocity field $\vec{U}'(x,y,z,t)$, which will in general be different from the velocity field $\vec{v}$ of the fluid. For such a moving surface of integration, the following kinematical theorem of Helmholtz, as given in reference 7, pp. 130-132, applies:

$$\frac{d}{dt} \iint \vec{A} \cdot \hat{n}\, dS = \iint \left[ \frac{\partial \vec{A}}{\partial t} + \vec{U}' \operatorname{div} \vec{A} - \operatorname{curl}\left( \vec{U}' \times \vec{A} \right) \right] \cdot \hat{n}\, dS \tag{8}$$

where $\vec{A}(x,y,z,t)$ is an arbitrary vector field. In this equation the flux of $\vec{A}$ through the moving and deforming surface S, given by $\iint \vec{A} \cdot \hat{n}\, dS$, is purely a function of time; hence, it is appropriate to take the total time derivative of this quantity as indicated in the first term of equation (8).

<div align="center">General Kinematic Form of the Vorticity-Flux Equation</div>

If the vector field $\vec{A}$ in Helmholtz' theorem is taken to be the vorticity $\vec{\omega} = \operatorname{curl} \vec{v}$, equation (8) becomes

$$\frac{d}{dt} \iint \vec{\omega} \cdot \hat{n}\, dS = \iint \left[ \frac{\partial \vec{\omega}}{\partial t} - \operatorname{curl}\left( \vec{U}' \times \vec{\omega} \right) \right] \cdot \hat{n}\, dS \tag{9}$$

Eliminating $\partial \vec{\omega}/\partial t$ between equations (7) and (9) yields the general kinematic form of the vorticity-flux equation

$$\frac{d}{dt} \iint \vec{\omega} \cdot \hat{n}\, dS + \iint \hat{n} \cdot \operatorname{curl} \left[ (\vec{U}' - \vec{v}) \times \vec{\omega} - \frac{1}{\rho} \operatorname{div} \overline{\overline{p}} + \frac{q}{\rho}(\vec{v} - \vec{v}^s) - 2\vec{v} \times \vec{\Omega} - \frac{\vec{f}}{\rho} \right] dS = 0 \tag{10}$$

where the surface of integration S is convected with the abstract velocity field $\vec{U}'(x,y,z,t)$. The abstract velocity field $\vec{U}'$ and the fluid velocity field $\vec{v}$ which appear in this equation may be regarded as superposed, $\vec{U}'$ governing the motion of the surface of integration S, and $\vec{v}$ the motion of the fluid elements. These two fields of motion are (in concept) unrelated. Equation (10) reduces to the usual form of the vorticity-flux relation in the special case of setting $\vec{U}' = \vec{v}$.

<div align="center">General Equation for Motion of Vorticity</div>

In relation (10) the abstract velocity $\vec{U}'$ with which the surface of integration S moves is continuous, but otherwise arbitrary. Now $\vec{U}'$ is constrained by the specification that S moves in such a manner that the flux of vorticity $\vec{\omega}$ through S is conserved; that is,

$$\frac{d}{dt} \iint \vec{\omega} \cdot \hat{n}\, dS = 0 \tag{11a}$$

The field $\vec{U}'$ when constrained in this manner is designated by the symbol $\vec{U}$, where $\vec{U}$ satisfies the equation

$$\iint \hat{n} \cdot \operatorname{curl} \left[ (\vec{U} - \vec{v}) \times \vec{\omega} - \frac{1}{\rho} \operatorname{div} \overline{\overline{p}} + \frac{q}{\rho}(\vec{v} - \vec{v}^s) - 2\vec{v} \times \vec{\Omega} - \frac{\vec{f}}{\rho} \right] dS = 0 \tag{11b}$$

Thus, $\vec{U}$ may be regarded as describing the motion of the vortex lines which pass through S.

Equation (12) applies to any surface of integration S having any chosen orientation, and the integrand is assumed to be continuous. This is possible only if

$$\text{curl}\left[\left(\vec{U} - \vec{v}\right) \times \vec{\omega} - \frac{1}{\rho} \text{div}\,\overleftrightarrow{p} + \frac{q}{\rho}\left(\vec{v} - \vec{v}^S\right) - 2\vec{v} \times \vec{\Omega} - \frac{\vec{f}}{\rho}\right] = 0 \qquad (12)$$

or, equivalently,

$$\boxed{\left(\vec{U} - \vec{v}\right) \times \vec{\omega} - \frac{1}{\rho} \text{div}\,\overleftrightarrow{p} + \frac{q}{\rho}\left(\vec{v} - \vec{v}^S\right) - 2\vec{v} \times \vec{\Omega} - \frac{\vec{f}}{\rho} = \text{grad}\,\phi} \qquad (13)$$

where $\phi(x,y,z,t)$ is an arbitrary scalar field.

Equation (13) is the desired general formula for the speed of displacement $\vec{U}$ of vorticity. Note that $\vec{U}$ is not, in general, determined uniquely because of the arbitrary function $\phi$. Physically, this means that for general distributions of vorticity there are arbitrarily many flux-preserving motions. In the simple case when $\vec{\omega} =$ Constant, any area-preserving motion of S perpendicular to $\vec{\omega}$ would also be flux conserving. But when a vortex tube is isolated, the displacement velocity $\vec{U}$ of the tube should be uniquely determined, except for displacements along the tube. $\left(\text{Also the term } \rho\,\text{grad}\,\phi \text{ may absorb forces directed along } \vec{\omega} \text{ which the term } \rho\left(\vec{U} - \vec{v}\right) \times \vec{\omega} \text{ cannot balance.}\right)$

Substituting equation (13) back into the momentum equation (5a) gives

$$\frac{\partial\vec{v}}{\partial t} - \vec{U} \times \vec{\omega} + \text{grad}\left(\frac{v^2}{2} - \Phi + \phi\right) = 0$$

or since in Cartesian coordinates

$$\text{grad}\,\frac{v^2}{2} = \left(\vec{v} \cdot \text{grad}\right)\vec{v} + \vec{v} \times \vec{\omega}$$

then

$$\left(\frac{\partial}{\partial t} + \vec{v} \cdot \text{grad}\right)\vec{v} = \left(\vec{U} - \vec{v}\right) \times \vec{\omega} + \text{grad}(\Phi - \phi) \qquad (14a)$$

which shows that the Magnus force density $\rho\left(\vec{U} - \vec{v}\right) \times \vec{\omega}$ acts directly to accelerate the fluid elements. Comparison with equation (5b) shows that in equation (14a), all the non-conservative forces, including the viscous force, are lumped together into one term and represented by the Magnus force density. The vorticity equation (6) becomes upon substitution of equation (13)

$$\frac{\partial \vec{\omega}}{\partial t} - \text{curl}\left(\vec{U} \times \vec{\omega}\right) = 0$$

or

$$\left(\frac{\partial}{\partial t} + \vec{U} \cdot \text{grad}\right)\vec{\omega} = \left(\vec{\omega} \cdot \text{grad}\right)\vec{U} - \vec{\omega} \text{ div } \vec{U} \tag{14b}$$

which is analogous $\left(\text{with } \vec{U} \text{ replacing } \vec{v}\right)$ to relations first obtained by Helmholtz under restrictive conditions. (See ref. 7, pp. 129-130.)

The pressure tensor $\vec{\vec{p}}$ has been retained for generality to illustrate that a displacement velocity $\vec{U}$ may be assigned to vortex tubes even in the presence of viscous diffusion. For an inviscid fluid, equation (13) becomes

$$\left(\vec{U} - \vec{v}\right) \times \vec{\omega} + \frac{1}{\rho} \text{grad } p + \frac{q}{\rho}\left(\vec{v} - \vec{v}^s\right) - 2\vec{v} \times \vec{\Omega} - \frac{\vec{f}}{\rho} = \text{grad } \phi \tag{15}$$

where p is the scalar pressure.

### Alternative Forms of the Vortex-Motion Equation

### for an Inviscid Fluid

The alternative formulas derived in this section are included here for completeness although they will not be used in subsequent sections. Because $\phi$ is arbitrary, any conservative terms on the left-hand side of equation (15) (i.e., terms which have the form of a gradient of some scalar quantity) may be deleted from the left-hand side and absorbed in the arbitrary grad $\phi$ term. Therefore, since

$$\frac{1}{\rho} \text{grad } p = \text{grad}\left(\frac{p}{\rho}\right) - p \text{ grad}\left(\frac{1}{\rho}\right) \tag{16}$$

equation (15) for an inviscid fluid can be expressed as

$$\left(\vec{U} - \vec{v}\right) \times \vec{\omega} - p \text{ grad}\left(\frac{1}{\rho}\right) + \frac{q}{\rho}\left(\vec{v} - \vec{v}^s\right) - 2\vec{v} \times \vec{\Omega} - \frac{\vec{f}}{\rho} = \text{grad } \phi \tag{17}$$

For an autobarotropic fluid, where pressure is a single-valued function of density (that is, $p = p(\rho)$), the term $\frac{1}{\rho} \text{grad } p$ in equation (15) and $p \text{ grad}\left(\frac{1}{\rho}\right)$ in equation (17) may be deleted by absorption into grad $\phi$. If, in addition, all nonconservative terms should be omitted, these equations become

$$\left(\vec{U} - \vec{v}\right) \times \vec{\omega} = \text{grad } \phi \tag{18}$$

from which it may be inferred by taking $\phi = 0$ that the components of $\vec{U}$ and $\vec{v}$ perpendicular to $\vec{\omega}$ are equal, in agreement with Kelvin's theorem that vorticity moves with the fluid under these conditions.

The density may be written

$$\rho = \rho'(p) + \rho'' \tag{19}$$

where $\rho'$ is a single-valued function of the pressure and $\rho''$ is the deviation of $\rho$ from $\rho'(p)$. It follows that

$$\frac{1}{\rho} = \frac{1}{\rho'(p)} - \frac{\rho''}{\rho\rho'(p)} \tag{20}$$

and equations (15) and (17) may be written, respectively,

$$\left(\vec{U} - \vec{v}\right) \times \vec{\omega} - \frac{\rho''}{\rho\rho'(p)} \operatorname{grad} p + \frac{q}{\rho}\left(\vec{v} - \vec{v}^{S}\right) - 2\vec{v} \times \vec{\Omega} - \frac{\vec{f}}{\rho} = \operatorname{grad} \phi \tag{21}$$

$$\left(\vec{U} - \vec{v}\right) \times \vec{\omega} + p \operatorname{grad}\left[\frac{\rho''}{\rho\rho'(p)}\right] + \frac{q}{\rho}\left(\vec{v} - \vec{v}^{S}\right) - 2\vec{v} \times \vec{\Omega} - \frac{\vec{f}}{\rho} = \operatorname{grad} \phi \tag{22}$$

where the terms $\frac{1}{\rho'(p)} \operatorname{grad} p$ and $p \operatorname{grad}\left[\frac{1}{\rho'(p)}\right]$ have been absorbed in the $\operatorname{grad} \phi$ term. Alternatively, if the pressure is written in the form

$$p = p'(\rho) + p'' \tag{23}$$

where $p'$ is a single-valued function of the density and $p''$ is the deviation of $p$ from $p'(\rho)$, equations (15) and (17) become, respectively,

$$\left(\vec{U} - \vec{v}\right) \times \vec{\omega} + \frac{1}{\rho} \operatorname{grad} p'' + \frac{q}{\rho}\left(\vec{v} - \vec{v}^{S}\right) - 2\vec{v} \times \vec{\Omega} - \frac{\vec{f}}{\rho} = \operatorname{grad} \phi \tag{24}$$

$$\left(\vec{U} - \vec{v}\right) \times \vec{\omega} - p'' \operatorname{grad}\left(\frac{1}{\rho}\right) + \frac{q}{\rho}\left(\vec{v} - \vec{v}^{S}\right) - 2\vec{v} \times \vec{\Omega} - \frac{\vec{f}}{\rho} = \operatorname{grad} \phi \tag{25}$$

From equation (13), (15), or (17) a speed of displacement $\vec{U}$ may be assigned to every element of vorticity in a fluid when the other relevant fields, such as pressure, density, and fluid velocity, are known. Evidently $\vec{U}$ frequently differs from $\vec{v}$. These equations may prove to be useful in forecasting the movement of severe local storms and

14

tropical storms. This is because they show explicitly how various atmospheric fields affect the movement of vorticity, and vorticity is a characteristic property of such storms. Conversely, they may aid in determining the structure of such atmospheric vortices from observations of their motion.

## Linearization of Equation for Vortex Motion

Perturbation series.- Analysis of equation (15) for the motion of vortex lines in an inviscid fluid is simplified by linearization as follows:

$$
\left.
\begin{aligned}
\vec{v} &= \vec{v}^0(x,y,z,t) + \epsilon \vec{v}^1(x,y,z,t) \\[6pt]
p &= p_0(x,y,z,t) + \epsilon p_1(x,y,z,t) \\[6pt]
\rho &= \rho_0(x,y,z,t) + \epsilon \rho_1(x,y,z,t) \\[6pt]
\phi &= \phi_0(x,y,z,t) + \epsilon \phi_1(x,y,z,t) \\[6pt]
\vec{\omega} &= \epsilon \vec{\omega}^1(x,y,z,t) \\[6pt]
q &= \epsilon q_1(x,y,z,t) \\[6pt]
\vec{f} &= \epsilon \vec{f}^1(x,y,z,t)
\end{aligned}
\right\}
\tag{26}
$$

where $\epsilon$ is a small dimensionless parameter. Substitution of set (26) in equation (15) gives for the unperturbed potential flow

$$
\frac{1}{\rho_0} \nabla p_0 - 2\vec{v}^0 \times \vec{\Omega} = \nabla \phi_0
\tag{27}
$$

From equation (5a) (with viscous terms omitted),

$$
\nabla \phi_0 = \nabla \left( \Phi_0 - \frac{v_0^2}{2} \right) - \frac{\partial \vec{v}^0}{\partial t}
\tag{28}
$$

where $\Phi_0$ is the potential for gravitational, centrifugal, and other conservative forces and $v_0^2 = \vec{v}^0 \cdot \vec{v}^0$. The first-order perturbation equation is

$$
\rho_0 \left( \vec{U} - \vec{v}^0 \right) \times \vec{\omega}^1 + q_1 \left( \vec{v}^0 - \vec{v}^s \right) + \nabla p_1 - 2\rho_0 \vec{v}^1 \times \vec{\Omega} - 2\rho_1 \vec{v}^0 \times \vec{\Omega} - \vec{f}^1 = \rho_0 \nabla \phi_1 + \rho_1 \nabla \phi_0
\tag{29}
$$

Substituting equation (27) in equation (29) gives

$$\rho_0\left(\vec{U} - \vec{v}^0\right) \times \vec{\omega}^1 + q_1\left(\vec{v}^0 - \vec{v}^s\right) + \nabla p_1 - \frac{\rho_1}{\rho_0}\nabla p_0 - 2\rho_0\vec{v}^1 \times \vec{\Omega} - \vec{f}^1 = \rho_0\nabla\phi_1 \tag{30}$$

For the present purposes it is desirable to simplify equation (30) further by eliminating the perturbation pressure $p_1$ and velocity $\vec{v}^1$ fields. The term $\nabla p_1/\rho_0$ may be absorbed into the $\nabla\phi_1$ term provided the unperturbed density $\rho_0$ is taken to be a constant. Elimination of $\vec{v}^1$ requires that the Coriolis force be neglected. With these two restrictions equation (30) becomes

$$\rho_0\left(\vec{U} - \vec{v}^0\right) \times \vec{\omega}^1 + q_1\left(\vec{v}^0 - \vec{v}^s\right) - \frac{\rho_1}{\rho_0}\nabla p_0 - \vec{f}^1 = \nabla\phi_1 \tag{31}$$

In many cases the arbitrary term $\nabla\phi_1$ in equation (31) may be set equal to zero. But in general it may be needed in order to balance forces directed parallel to the vortex lines, which the Magnus term $\rho_0\left(\vec{U} - \vec{v}^0\right) \times \vec{\omega}^1$ cannot balance.

Physical interpretation of terms in linearized equation for vortex motion.- The terms of equation (31) all have the dimensions of force per unit volume. The first term $\rho_0\left(\vec{U} - \vec{v}^0\right) \times \vec{\omega}^1$ represents the Magnus force density on vortex filaments which do not move with the unperturbed flow velocity $\vec{v}^0$. The second term $q_1\left(\vec{v}^0 - \vec{v}^s\right)$ represents the force density required to accelerate the source fluid from the source velocity $\vec{v}^s$ to the flow velocity $\vec{v}^0$. The third term $\frac{\rho_1}{\rho_0}\nabla p_0$ represents a "buoyancy" force which acts on density variations in the presence of the unperturbed pressure gradient. It corresponds, for example, to the buoyant lift on a balloon. The fourth term $\vec{f}^1$ represents an extraneous, nonconservative force density, which in this study will be taken to be the magnetic force density $\vec{f}^1 = \vec{j}^1 \times \vec{B}^0$ where $\vec{j}^1$ is a perturbation electric current density, and $\vec{B}^0$ is the applied magnetic field.

Equation (31) states that the vorticity moves in such a manner that the Magnus force, source-force, buoyant-force, and magnetic-force densities vanish (or are equal to the gradient of some scalar field). Only the Magnus term $\rho_0\left(\vec{U} - \vec{v}^0\right) \times \vec{\omega}^1$ contains the velocity of displacement $\vec{U}$ of the vorticity. Incidentally, in the derivation of equation (31) no attempt has been made to follow the motion of any quantity except the vorticity. That is, source strength is not necessarily conserved and density irregularities are not necessarily followed by the motion $\vec{U}$.

Linearized equation for the motion of isolated vortex tubes.- Up to this point the vorticity has been considered to be distributed generally throughout the flow. The case of an isolated vortex tube of circulation $\Gamma$ will now be considered as a prelude to the

treatment of atmospheric vortices. For application of equation (31) to an isolated vortex tube, it is convenient to integrate over the volume $V$ of the tube included between two surfaces $S'$ and $S''$ which are everywhere normal to the vorticity in the tube, as shown in figure 2.
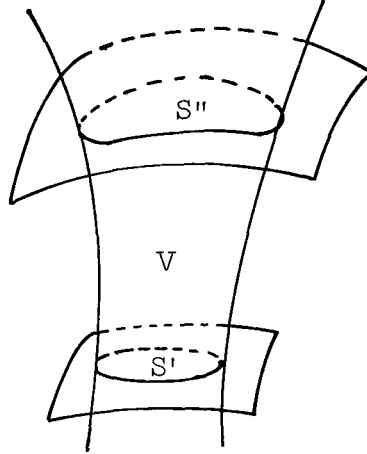


Figure 2.- Isolated vortex tube with cross-sectional surfaces $S'$ and $S''$ and included volume $V$ shown.

Upon integration, equation (31) becomes

$$\iiint \left[ \rho_o (\vec{U} - \vec{v}^o) \times \vec{\omega}^1 + q_1 (\vec{v}^o - \vec{v}^s) - \frac{\rho_1}{\rho_o} \nabla p_o - \vec{f}^1 - \nabla \phi_1 \right] dV = 0 \tag{32}$$

This volume integral may be written as an integral on a cross-sectional surface $S$ and along a line $l$ parallel to the vorticity:

$$\int dl \iint dS \left[ \rho_o (\vec{U} - \vec{v}^o) + q_1 (\vec{v}^o - \vec{v}^s) - \frac{\rho_1}{\rho_o} \nabla p_o - \vec{f}^1 - \nabla \phi_1 \right] = 0 \tag{33}$$

Since the integrand is assumed to be continuous throughout $V$, mean values may be assigned to the quantities $(\vec{U} - \vec{v}^o)$, $(\vec{v}^o - \vec{v}^s)$, $\nabla p_o$, and $\nabla \phi_1$ on surface $S$ so that equation (33) is termwise identical with the following equation:

$$\int dl \left[ \rho_o \langle \vec{U} - \vec{v}^o \rangle \times \iint \vec{\omega}^1 dS + \langle \vec{v}^o - \vec{v}^s \rangle \iint q_1 dS - \frac{\langle \nabla p_o \rangle}{\rho_o} \iint \rho_1 dS \right.$$

$$\left. - \iint \vec{f}^1 dS - \langle \nabla \phi_1 \rangle \iint dS \right] = 0 \tag{34}$$

where the brackets $\langle \ \rangle$ denote mean values on the cross-sectional surface $S$. This

17

equation may also be written

$$\int \left[ \rho_o \left\langle \vec{U} - \vec{v}^o \right\rangle \times \vec{\Gamma}^1 + \left\langle \vec{v}^o - \vec{v}^s \right\rangle Q_1 - \frac{\left\langle \nabla p_o \right\rangle}{\rho_o} M_1 - \vec{F}^1 - \left\langle \nabla \phi_1 \right\rangle A \right] d\ell = 0 \qquad (35)$$

where

$\vec{\Gamma}^1$          circulation of the vortex tube

$Q_1$          mass of source fluid being added to the vortex tube per unit length

$M_1$          excess mass present in the tube per unit length

$\vec{F}^1$          Lorentz force on the tube per unit length

$A$          cross-sectional area of the tube (taken perpendicular to $\vec{\omega}^1$)

The remaining integration in equation (35) is over an arbitrary length $\ell$ of the vortex tube, and the integrand is assumed to be a continuous function of $\ell$; hence, the integrand itself must vanish for all values of $\ell$:

$$\rho_o \left\langle \vec{U} - \vec{v}^o \right\rangle \times \vec{\Gamma}^1 + \left\langle \vec{v}^o - \vec{v}^s \right\rangle Q_1 - \frac{\left\langle \nabla p_o \right\rangle}{\rho_o} M_1 - \vec{F}^1 = \left\langle \nabla \phi_1 \right\rangle A \qquad (36)$$

The arbitrary term $\left\langle \nabla \phi_1 \right\rangle A$ has been retained for the purpose of balancing possible axial forces which cannot be balanced by the Magnus force $\rho_o \left\langle \vec{U} - \vec{v}^o \right\rangle \times \vec{\Gamma}^1$. This first-order perturbation equation is applicable to an isolated weak vortex tube in an inviscid fluid without Coriolis forces. The unperturbed flow must be irrotational and free of sources, have constant density $\rho_o$, and must satisfy the equation

$$\frac{\nabla p_o}{\rho_o} = \nabla \left( \Phi_o - \frac{v_o^2}{2} \right) - \frac{\partial \vec{v}^o}{\partial t} \qquad (37)$$

where $\Phi_o$ is the potential for gravitational, centrifugal, and other conservative forces.

In subsequent sections where equation (36) is applied, the subscript 1 (or superscript 1) will be dropped from the perturbation fields $\vec{\Gamma}^1$, $Q_1$, $M_1$, and $\vec{F}^1$. The subscipt o (or superscript o) will be retained on the unperturbed fields, however. Any confusion which might arise from this practice can be resolved by referring back to equation (36).

# APPLICATIONS OF LINEARIZED EQUATION FOR VORTEX MOTION

## TO TORNADOES AND TORNADO CYCLONES

### Rudimentary Approach To Be Used in the Following Applications

In the following sections equation (36) will be applied to tornadoes and tornado cyclones as if they were weak perturbations on an unperturbed potential flow. All non-linear effects will clearly be missing in this rudimentary treatment. Moreover, only gross features of these storms, such as circulation, updraft, and core density, will be considered together with some effects of the boundary layer at the ground and of the jet stream near the tropopause.

This simplified version of a severe local storm which is producing a tornado may be described briefly as follows:[1] A tornado cyclone, or parent storm, is regarded as a vertical vortex which significantly affects the flow in a region about 16 km (10 miles) in diameter. The tornado cyclone has a core that is several miles in diameter and a strong updraft within the core. The cyclone terminates near the tropopause and the updraft from its core is ejected into the jet stream and carried eastward. A tornado produced by this storm is pendent from the cloud base at an altitude on the order of 0.3 km (1000 ft) and may extend to the ground. The circulation of the tornado is about 1 order of magnitude less than that of the tornado cyclone, and its core diameter is from 1 to 2 orders of magnitude less. An updraft exists in the tornado core, and retarded fluid from the viscous boundary layer at the ground is drawn up into the tornado. This interaction with the boundary layer at the ground is considered capable of affecting the speed of displacement of the lower portion of the tornado — but not of the tornado cyclone. The motion of the tornado cyclone, however, may be influenced by its inter-action with the jet stream above. Since the boundary layer at the ground acts as a source, and the jet stream acts as a sink, both these effects depend upon the source term $\left\langle \vec{v}^O - \vec{v}^S \right\rangle Q_1$ in equation (36), and these are the first cases which will be treated.

Because of the high speed of the circulating wind in a tornado, the tornado core may be rarefied so that its motion is influenced by the buoyancy term $\dfrac{\left\langle \nabla p_o \right\rangle}{\rho_o} M_1$ in equa-tion (36). Also, the updrafts in a tornado cyclone indicate that the core of the cyclone may be warmer than the surrounding air and therefore buoyant. If the vortices should be tilted from the vertical, one effect of their buoyancy would be the presence of upward lift, which could affect their motion. This effect, although potentially important, will be omitted in the case of the twin tornado because the algebra becomes cumbersome. It will also be omitted from the treatment of tornado cyclones because it appears that in this

---

[1]For a more complete discussion of severe local storms, see reference 2.

case the term $\nabla p_1$ in equation (30) cannot be absorbed into the $\rho_0 \nabla \phi_1$ term, as done throughout this report, nor can it be ignored. The case of buoyancy which will be treated with equation (36) is that of buoyant attraction between the rarefied cores of a twin tornado.

The applications of equation (36) are concluded with a hypothetical example which depends upon the Lorentz term. The case treated is that of two parallel vortices which are subject to magnetic attraction by virtue of dc axial electric currents of like sense in the vortex cores.

### Effect of the Boundary Layer at the Ground on Tornado Motion

Description and analysis.- For this analysis the following simplified form of equation (36) is used:

$$\rho_0 \left\langle \vec{U} - \vec{v}^0 \right\rangle \times \vec{\Gamma} + \left\langle \vec{v}^0 - \vec{v}^s \right\rangle Q = 0 \tag{38}$$

where only the Magnus term and source term have been retained, and where the subscript 1 (or superscript 1) has been dropped from the perturbation fields $\Gamma$ and $Q$. Near the ground the flow undergoes a rapid transition from the free-stream flow to the retarded flow in the viscous boundary layer. Ordinarily, the boundary layer does not significantly affect the free-stream flow. But in the event of a tornado, the retarded fluid in the boundary layer is sucked up into the free stream as shown in figure 3(a). This constitutes a fluid source at the boundary of the free stream, which is coincident with the tornado and can affect its motion.

The upward flux of fluid from the boundary layer into the tornado core occurs essentially as follows: The pressure $p$ in the boundary layer is the same as in the free stream, although the flow is considerably retarded. Therefore the radial pressure gradient within the free-stream vortex also exists in the boundary layer below. The boundary-layer fluid moves radially inward under the influence of this pressure gradient and ultimately ascends into the low-pressure tornado core. Although the magnitude of this flux from the boundary layer to the free stream may not be accurately known, there is ample evidence of its existence (ref. 12, p. 675, and ref. 3, p. 7).

This upward flux of fluid from the boundary layer appears as a source to the free stream. The total magnitude of this source, in kg/sec, is

$$\mathcal{Q} = \rho_0 A v_1 \tag{39}$$

where $A$ is the area of the tornado core at the free-stream boundary, and $v_1$ is the upward component of velocity at this boundary. The fluid source is located (concentrated)

on the lower boundary of the free stream.  From equation (38), therefore, a strong displacement, or kink, would be expected to develop in the tornado at this boundary.  But observation of tornadoes indicates that this does not occur and that the tornado maintains
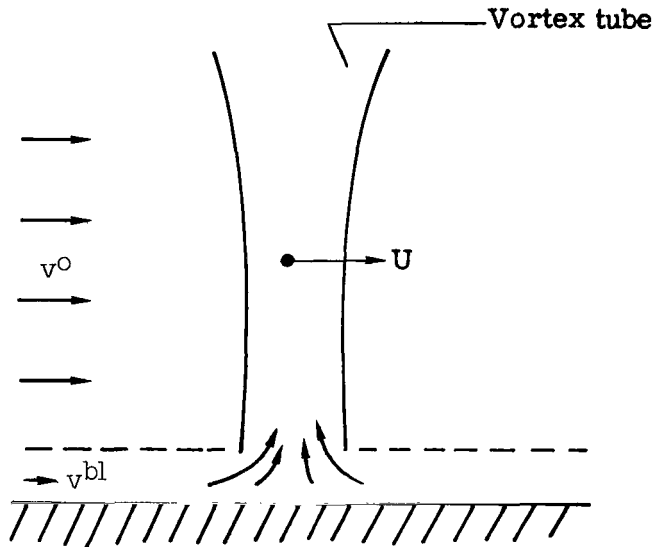


(a) Vortex tube drawing fluid up from the boundary layer.
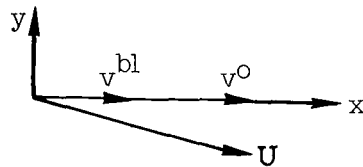


(b) Top view of displacement velocity $\vec{U}$ of vortex tube relative to the
free-stream velocity $\vec{v}^o$ and the boundary-layer velocity $\vec{v}^{bl}$.

Figure 3.- Effect on vortex motion of the boundary layer at the ground.

a smooth contour, as if the source were distributed over a finite length of the vortex tube instead of being concentrated at its lower extremity.  It may be that there is a stabilizing effect in the tornado which acts to prevent strong curvature of the core, and in so doing, effectively distributes the concentrated source.

Such a stabilizing effect is assumed to exist and the source strength $Q$ is considered to be distributed over a vertical length  L  of the lower part of the tornado, whence

$$Q = \frac{\rho_o A v_1}{L}$$

(40)

21

and equation (38) becomes

$$\left(\vec{U} - \vec{v}^o\right) \times \vec{\Gamma} + \left(\vec{v}^o - \vec{v}^{bl}\right)\frac{Av_\perp}{L} = 0 \tag{41}$$

where $\vec{v}^{bl}$ is the unperturbed velocity in the boundary layer (source fluid), and where the brackets have been dropped by taking mean values over the vortex cross section to be approximated by values at the core center. If

$$\vec{v}^{bl} = c\vec{v}^o \tag{42}$$

with $0 < c < 1$, then

$$\left(\vec{U} - \vec{v}^o\right) \times \vec{\Gamma} + \vec{v}^o(1 - c)\frac{Av_\perp}{L} = 0 \tag{43}$$

In Cartesian component form, with circulation $\vec{\Gamma}$ taken along the z-axis and $\vec{v}^o$ taken in the x-direction, equation (43) becomes

$$U_y\Gamma + v^o(1 - c)\frac{Av_\perp}{L} = 0 \tag{44a}$$

$$\left(U_x - v^o\right)\Gamma = 0 \tag{44b}$$

whence

$$U_x = v^o \tag{45a}$$

$$U_y = -v^o(1 - c)\frac{Av_\perp}{\Gamma L} \tag{45b}$$

It is clear from equations (45) that the effect of the boundary layer at the ground is to make the base of the funnel move to the right of the local wind $\vec{v}^o$, as shown in figure 3(b). In the case of the twin tornado referred to in the Introduction and in appendix B, this implies that the lower portions of the two funnels should tend to separate as they revolve about each other. According to figure 4, which was prepared by Fujita (ref. 4), they did apparently separate from a center-to-center distance of 118.9 m (390 ft) to 147.1 m (482.6 ft) in a period of 52 sec during which time the pair revolved about their common center through an angle of about $140^o$.
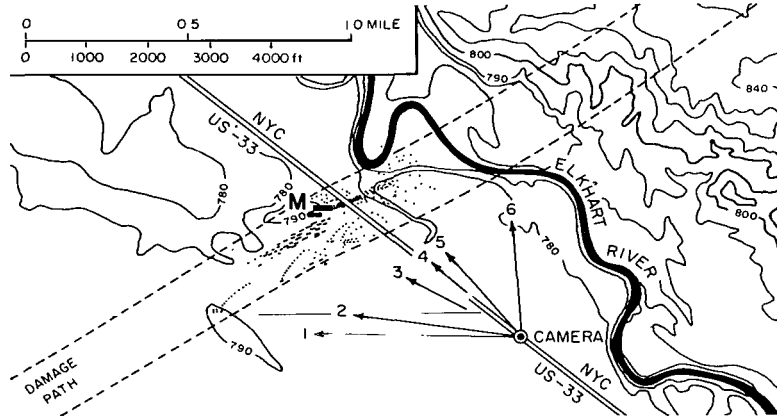
(a) Damage path and debris marks near the Midway Trailer Court indicated by letter M. Six pictures were taken in the direction of the arrows.
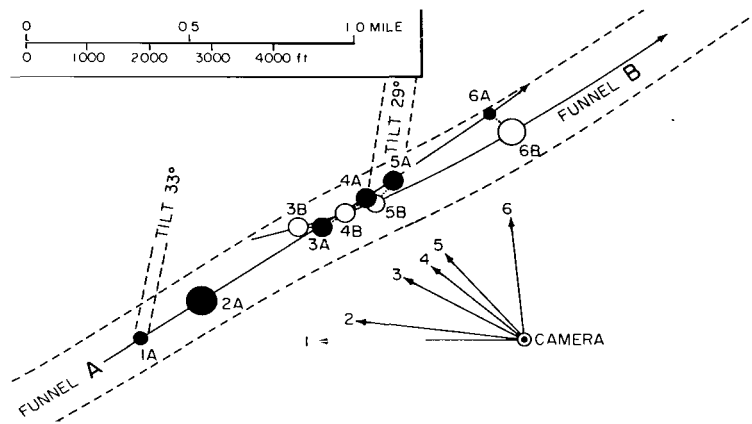


(b) Sequence depicting the initial occurrence of funnel A, the subsequent occurrence and growth of funnel B at the expense of funnel A, and the revolution of funnels A and B about their common center.
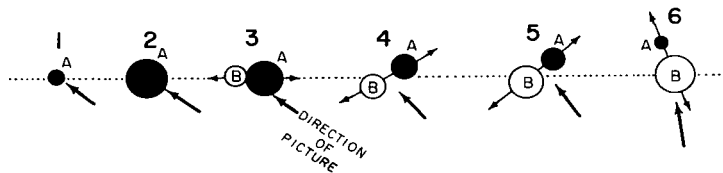


(c) Photogrammetric sketches of the tornado pair.

Figure 4.- Twin tornado J-2 path and configuration, as drawn by Fujita (ref. 4) from an aerial survey and from the six photographs taken by Paul Huffman.

Order-of-magnitude check on boundary-layer effect.- In order to check whether the observed rate of separation of the twin tornado could possibly have been due to boundary-layer interaction, an order-of-magnitude calculation for this effect may be made as follows: For the tornado pair the ratio of radial speed of displacement $-U_y$ to tangential speed of displacement $U_x$ is on the order of $-U_y/U_x \approx 0.1$. From equations (45),

$$\frac{-U_y}{U_x} = (1 - c)\frac{Av_\perp}{\Gamma L} \approx 0.1$$

or

$$v_\perp = \frac{\Gamma L}{A(1 - c)} \times 0.1 \tag{46a}$$

A value for A, the area of the core at the base of one of the funnels, may be obtained from figure 5

$$A = 6 \times 10^3 \text{ m}^2$$

where the scale length used in this estimate is the center-to-center distance as given in table I, location 4. The circulation $\Gamma$ of each funnel, when approximately equal in strength at location 4, is estimated in appendix C as

$$\Gamma \approx 5 \times 10^3 \text{ m}^2/\text{sec}$$

Taking the mean velocity in the boundary layer equal to one-half the free-stream velocity gives, from equation (42),

$$c = 0.5$$

When these values for A, $\Gamma$, and c are substituted, equation (46a) becomes

$$v_\perp = \frac{L}{6} \tag{46b}$$

which is a relation between the updraft velocity $v_\perp$ in the core at the boundary layer and the length L at the base of each funnel, which is assumed to be affected by the boundary-layer interaction. Taking L = 60 m (196 ft) gives $v_\perp$ = 10 m/sec (22.4 mph) for the updraft velocity at the boundary layer, a value which appears to be of reasonable magnitude. It is concluded that the increasing separation observed for the twin tornado may have been due to its interaction with the boundary layer at the ground.

Figure 5.- Photograph of twin tornado J-2 taken at 5:30 p.m. CST on April 11, 1965; number 4 of a series of six pictures taken by Paul Huffman, staff photographer of the Elkhart Truth. Left funnel is shown over the Midway Trailer Court (fig. 20). Reproduced by permission.

## Effect of the Jet Stream on Motion of Tornado Cyclones

The jet stream as a sink fluid.- In this section, equation (36) is again considered in the simplified form of equation (38)

$$\rho_o \left\langle \vec{U} - \vec{v}^o \right\rangle \times \vec{\Gamma} + \left\langle \vec{v}^o - \vec{v}^s \right\rangle Q = 0$$

where all terms except the Magnus term and source term are neglected. When a thunderstorm matures into a severe storm, which may generate tornadoes and hail, the storm cell begins to rotate cyclonically (in the northern hemisphere) according to observations reported in reference 3, pp. 3-4. This vortex is termed a "tornado cyclone." In addition to circulation, there is a strong axial flow of rising air within the vortex which frequently penetrates the tropopause. In the vicinity of the tropopause at midlatitudes is a narrow band of high-speed flow called the jet stream (ref. 13, p. 553). Much of the fluid in the

25

updraft of the storm is swept eastward by the jet stream as shown in figure 6, and forms the broad anvil canopy which is characteristic of these storms (ref. 1, pp. 67-68, and ref. 2, pp. 185-195). For the tropospheric flow below, therefore, the jet stream constitutes a sink fluid.
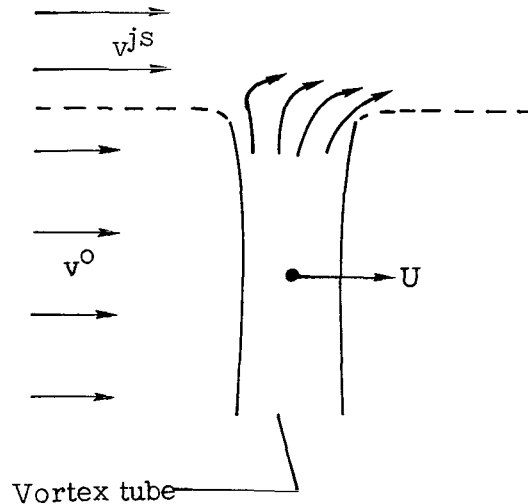


Figure 6.- Vortex tube ejecting fluid into the jet stream.

The efflux of fluid from the tornado cyclone into the jet stream will affect the motion of the tornado cyclone in the troposphere below the jet stream. In particular, an attempt will be made to show on the basis of equation (38) that the storm will tend to move to the right of the mean winds in the troposphere in agreement with observations reported in reference 1, pp. 71-72, and reference 2, pp. 319-321.

The winds in the troposphere below the jet stream vary considerably in direction with altitude, as described in reference 2, pp. 319-336. Moreover, the actual location of the fluid sink is near the upper extremity of the storm, where the cyclone core intersects the lower boundary of the jet stream. Despite the wind variation and sink concentration, the storms are observed to move, more or less, as a unit, although the core of the storm may be tilted from the vertical by as much as $20^{\circ}$ (ref. 1, p. 69). Possibly the storm structure resists deformation of the core of the cyclone and in so doing effectively spreads out localized effects over its entire vertical extent. If this is the case, it would seem appropriate to distribute the sink strength uniformly over the vertical extent $L$ of the storm and also to define a mean wind velocity $\vec{v}^{o}$ for the troposphere below the jet stream. This is the view which is adopted in this section. The vortex tube is also assumed to flare out horizontally upon penetrating the jet stream so that the tube as such is confined to the flow region below the jet stream.

The total strength of the sink is $\rho_0 Av_\perp$, which in terms of total source strength in kg/sec is

$$\mathcal{Z} = -\rho_o A v_\perp \tag{47}$$

where $A$ is the cross-sectional area of the rising column of fluid at the lower jet-stream boundary and $v_\perp$ is its upward velocity at the boundary. When this source strength is distributed over the height $L$ of the vortex, the source strength per unit length is

$$Q = -\frac{\rho_o A v_\perp}{L} \tag{48}$$

and equation (38) becomes

$$\left(\vec{U} - \vec{v}^o\right) \times \vec{\Gamma} - \left(\vec{v}^o - \vec{v}^{js}\right)\frac{A v_\perp}{L} = 0 \tag{49}$$

where $\vec{v}^{js}$ is the fluid velocity in the jet stream (sink fluid) and $\vec{v}^o$ is the mean fluid velocity in the troposphere below. The brackets are eliminated in equation (49) by taking the mean values over the vortex-core cross section to be approximated by values at the core center. If $\vec{v}^o$ is taken along the x-axis of a Cartesian coordinate system and $\vec{\Gamma}$ along the z-axis, equation (49) becomes in component form

$$U_y \Gamma - \left(v^o - v_x^{js}\right)\frac{A v_\perp}{L} = 0 \tag{50a}$$

$$\left(U_x - v^o\right)\Gamma - v_y^{js}\frac{A v_\perp}{L} = 0 \tag{50b}$$

whence

$$U_x = v^o + v_y^{js}\frac{A v_\perp}{\Gamma L} \tag{51a}$$

$$U_y = \left(v^o - v_x^{js}\right)\frac{A v_\perp}{\Gamma L} \tag{51b}$$

Sample solutions for the motion of tornado cyclones.- The dimensionless constant $A v_\perp/\Gamma L$ in equations (51) may be estimated by using the following typical values: Circulation of the tornado cyclone (ref. 1, p. 76),

$$\Gamma = 10^5 \ m^2/sec \tag{52a}$$

Vertical extent of storm (ref. 2, pp. 176-177),

$$L = 12.2 \text{ km} \quad (40\ 000 \text{ ft}) \tag{52b}$$

Upward velocity of fluid in the cyclone core (ref. 12, p. 675),

$$v_{\perp} = 152 \text{ m/sec} \quad (500 \text{ ft/sec}) \tag{52c}$$

Area of core, assumed circular with radius $\sqrt{2}$ km (ref. 1, p. 74),

$$A = 6.28 \times 10^6 \text{ m}^2 \tag{52d}$$

The resultant value for the dimensionless constant is

$$\frac{Av_{\perp}}{\Gamma L} = 0.78 \tag{53}$$

In order to determine the storm displacement velocity $\vec{U}$, two other quantities must be specified in equations (51). These are the ratio $v^{js}/v^o$ of the wind magnitude in the jet stream $v^{js}$ to that below $v^o$, and the included angle between $\vec{v}^o$ and $\vec{v}^{js}$. (In the vector diagrams of figure 7, the vortex is viewed from above and $\vec{v}^o$ is always taken to lie in the same direction.) In figure 7(a), the wind-speed ratio is $\dfrac{v^{js}}{v^o} = \dfrac{3}{2}$ and vector diagrams are sketched for various included angles between $\vec{v}^o$ and $\vec{v}^{js}$ in $15^o$ increments. Similar diagrams are presented in figure 7(b) for $\dfrac{v^{js}}{v^o} = \dfrac{2}{1}$. Note that the speed-of-displacement vector $\vec{U}$ is usually found to lie to the right of both $\vec{v}^o$ and $\vec{v}^{js}$ in agreement with observation. The general condition that $\vec{U}$ lie to the right of $\vec{v}^o$ is that $\left(\vec{v}^{js} - \vec{v}^o\right) \cdot \vec{v}^o > 0$.

### Effect of Core Buoyancy on Revolution Rate of a Twin Tornado

Occurrence of twin tornado J-2.- On April 11, 1965, a twin tornado (fig. 5) occurred near Elkhart, Indiana. Full details of this tornado (designated J-2) are presented in reference 4, and an abbreviated account is given in appendix B of this paper. The funnels were parallel, about 122 m (400 ft) apart (center-to-center distance), and were tilted at an angle of about $29^o$ from the vertical. Their circulations were of like sense (cyclonic) and they revolved about each other while slightly increasing the distance of separation. The relative motion of this tornado pair is an interesting case to which equation (13) should apply. Rather than attempt this at present, the linearized form, equation (36), will be applied, despite its limitation to weak vortices in an inviscid fluid without Coriolis forces.
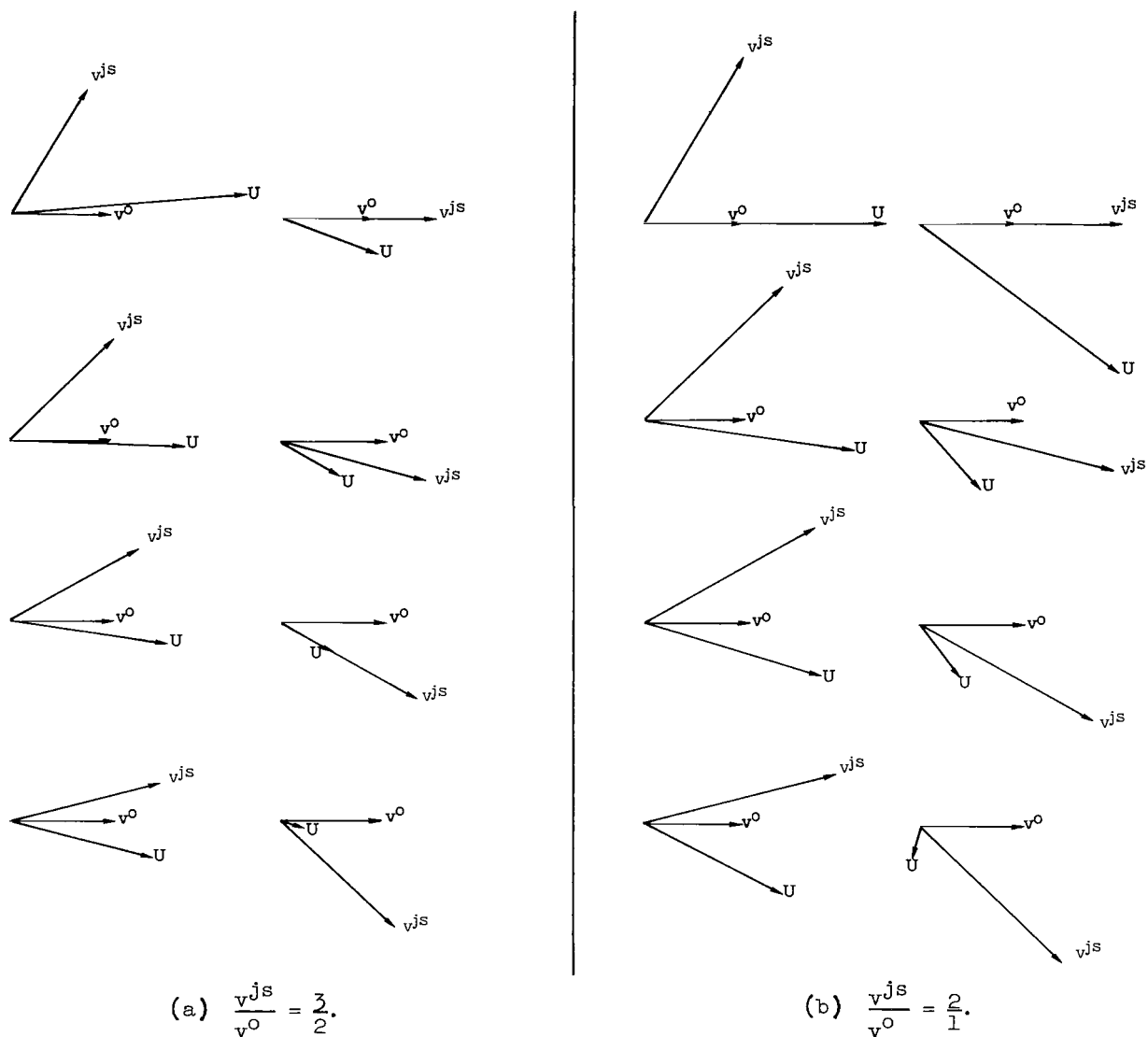
28

Figure 7.- Top views of displacement velocity $\vec{U}$ of tornado cyclone relative to free-stream velocity $\vec{v}^o$ and jet-stream velocity $\vec{v}^{js}$ for different orientations of $\vec{v}^{js}$.

Tornado model.- Figure 8 depicts a physical model for the twin tornado to which equation (36) may be applied. The vorticity is assumed to be largely contained in two tubes which are finite in cross section, semi-infinite in length, and terminate at the ground. The tubes are parallel, but tilted with respect to the vertical, and do not necessarily have the same circulation strength. Updrafts are present within the cores as an outlet for the convergent flow in the boundary layer at the ground, which was mentioned in the section entitled "Effect of the Boundary Layer at the Ground on Tornado Motion."
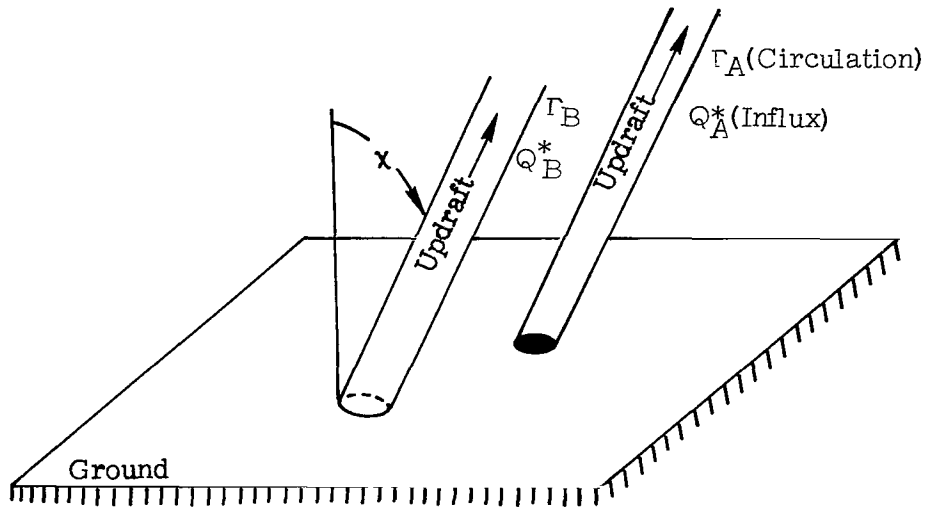
Figure 8.- Model used for twin tornado:  tilted vortex tubes with updraft and influx.

One model for tornadoes (refs. 14 and 15) assumes that such a convergent flow exists not only within the boundary layer at the ground, but at every point along the vertical extent of the funnel in the free stream.  This convergent flow is conceived as maintaining the concentration of vorticity in the funnels.  Thus besides circulation  $\Gamma$, each core has convergence  $Q^*$, in kg/m-sec, which represents the rate at which convergent fluid is entering the core per unit length in the free stream.  The asterisk notation is needed because within the core this convergent flow of fluid turns upward in a rising column which remains a part of a total free-stream flow field.  If the converging fluid were actually withdrawn from the flow (as by entering a pipe), the asterisk notation would be unnecessary.

This circulation-convergence-updraft model will be adapted herein for tornadoes. Thus the cores in figure 8 are assigned individual circulations  $\Gamma_A$  and  $\Gamma_B$  and convergences  $Q^*_A$  and  $Q^*_B$.  For a given location of the tubes the velocity field  $\vec{v}$  outside the cores may be solved for, assuming that the external fluid is inviscid, incompressible, and irrotational, and that it does not penetrate the ground.  The velocity field thus determined should be a good approximation to the real flow except within the cores and within the boundary layer at the ground.  The effect of the boundary layer at the ground, which is to make the cores move to the right of the local flow (and thus tend to separate) has already been discussed in the section entitled "Effect of the Boundary Layer at the Ground on Tornado Motion."

Absence of source force density despite possible convergent flow.- The motion of the cores may be determined from equation (36).  The source term  $\langle \vec{v}^O - \vec{v}^S \rangle Q$  in this equation would apply if  $Q^*_A$  and  $Q^*_B$  were true sinks.  However, they are fictitious in

that the converging fluid is not withdrawn from the free-stream flow, but is simply deflected upward. This rising column does not constitute a sink except at a point where it penetrates through a surface of discontinuity into a different flow region. Any such penetration point is assumed to occur only at altitudes which are large compared with the separation distance of the two tornadoes, so that the relative motion of the two funnels near the ground is unaffected by it. Therefore, despite convergence in the tornado model, the source term $\langle \vec{v}^O - \vec{v}^S \rangle Q$ in equation (36) is properly equated to zero for this study of the mutual interaction between the funnels.

Buoyancy terms.- Now if the Lorentz force density $\vec{F}$ in equation (36) is also not considered, the buoyancy term $\dfrac{\langle \nabla p_O \rangle}{\rho_O} M$ remains to influence the motion of the vortex pair:

$$\rho_O \langle \vec{U} - \vec{v}^O \rangle \times \vec{\Gamma} - \frac{\langle \nabla p_O \rangle}{\rho_O} M = A \langle \nabla \phi \rangle \tag{54}$$

The possibility exists that the cores of the tornado pair are partially rarefied. This will occur if the circulating winds approach the speed of sound near the cores, as illustrated in the compressible-vortex example presented in reference 10, pp. 158-159. Thus the excess mass $M$ per unit length is negative, and each vortex is buoyant in the radial pressure gradient of the flow field of the other. Consequently, the buoyancy force acting upon the pair should be attractive and tend to slow down their revolution rate.

Effect of tilt neglected.- Although the convergences $Q_A^*$ and $Q_B^*$ do not appear explicitly in equation (54), they still influence the velocity fields and pressure gradients in this equation and thus complicate the solution. The problem of two buoyant vortices with influx is simplified if the pair are taken to be alined with the vertical and to be identical in influx and circulation, as illustrated in figure 9 where $\Gamma_A = \Gamma_B = \Gamma$ and $Q_A^* = Q_B^* = Q^*$. The equal influx and circulation strengths correspond to the state of the tornado pair at location 4 of figure 4. Neglecting the tilt angle appears to be warranted in the following order-of-magnitude calculation to determine whether buoyant attraction could cause signficant retardation in the revolution rate of twin vortices with influx. In appendix C it is estimated that the revolution rate of the twin tornado was retarded by at least 50 percent with respect to the fluid.

Adaptation of linearized equation for vortex motion to twin-vortex model.- In order to calculate the motion $\vec{U}^A$ of vortex A, the unperturbed flow, represented by $\vec{v}^O$ and $p_O$ in equation (54), is taken to be the flow field due to vortex B. Similarly, the motion of vortex B is determined by considering the unperturbed flow to be that due to
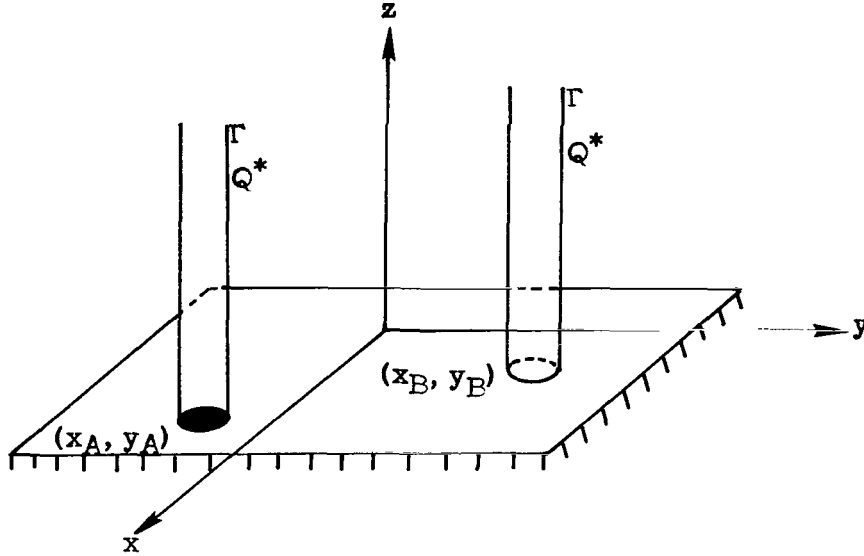
Figure 9.- Vertical vortex tubes having identical circulation and influx with centers at $\left(x_A, y_A\right)$ and $\left(x_B, y_B\right)$.

vortex A. For either vortex equations (54) and (37) apply:

$$\rho_0 \left\langle \vec{U} - \vec{v}^0 \right\rangle \times \vec{\Gamma} - M \left\langle \nabla \left( \Phi_0 - \frac{v_0^2}{2} \right) - \frac{\partial \vec{v}^0}{\partial t} \right\rangle = A \left\langle \nabla \phi \right\rangle \tag{55}$$

where $v_0^2 = \vec{v}^0 \cdot \vec{v}^0$. In the Cartesian coordinate system of figure 9 where the z-axis is vertical, the x- and y-components of equation (55) are, for vertical vortices,

$$\frac{\rho_0 \Gamma_z}{M} \left( U_y - v_y^0 \right) + v_x^0 \frac{\partial v_x^0}{\partial x} + v_y^0 \frac{\partial v_y^0}{\partial x} + \frac{\partial v_x^0}{\partial t} = 0 \tag{56a}$$

$$-\frac{\rho_0 \Gamma_z}{M} \left( U_x - v_x^0 \right) + v_x^0 \frac{\partial v_x^0}{\partial y} + v_y^0 \frac{\partial v_y^0}{\partial y} + \frac{\partial v_y^0}{\partial t} = 0 \tag{56b}$$

where the brackets have been eliminated by taking the mean values over the vortex cores to be approximated by values at the core centers. The $A \left\langle \nabla \phi \right\rangle$ term was retained in equation (55) only for the purpose of balancing possible axial forces. For vertical vortices this term need have only a z-component and therefore does not appear in equations (56).

Suppose now that the vortex giving rise to the unperturbed flow is located at the moving point $x_m(t), y_m(t)$. The velocity components for the unperturbed flow are then given by

$$v_x^o = \frac{K(x - x_m)}{|\vec{r} - \vec{r}_m|^2} - \frac{G(y - y_m)}{|\vec{r} - \vec{r}_m|^2}$$

$$v_y^o = \frac{K(y - y_m)}{|\vec{r} - \vec{r}_m|^2} + \frac{G(x - x_m)}{|\vec{r} - \vec{r}_m|^2}$$

(57)

where

$$K = \frac{Q^*}{2\pi}$$

$$G = \frac{\Gamma}{2\pi}$$

$$|\vec{r} - \vec{r}_m| = \sqrt{(x - x_m)^2 + (y - y_m)^2}$$

These velocity fields and their x-, y-, and t-derivatives, if evaluated on the line $y - y_m = 0$, take the form

$$v_x^o = \frac{K}{(x - x_m)}$$

(58a)

$$\frac{\partial v_x^o}{\partial x} = - \frac{K}{(x - x_m)^2}$$

(58b)

$$\frac{\partial v_x^o}{\partial y} = - \frac{G}{(x - x_m)^2}$$

(58c)

$$\frac{\partial v_x^o}{\partial t} = \frac{\dot{x}_m K}{(x - x_m)^2} + \frac{\dot{y}_m G}{(x - x_m)^2}$$

(58d)

$$v_y^o = \frac{G}{(x - x_m)}$$

(58e)

$$\frac{\partial v_y^o}{\partial x} = - \frac{G}{(x - x_m)^2}$$

(58f)

$$\frac{\partial v_y^o}{\partial y} = \frac{K}{(x - x_m)^2}$$

(59g)

33

$$\frac{\partial v_y^o}{\partial t} = \frac{\dot{x}_m G}{\left(x - x_m\right)^2} - \frac{\dot{y}_m K}{\left(x - x_m\right)^2} \tag{58h}$$

where dots denote time derivatives, and where $K$ and $G$ are taken to be constants.

Now take the two moving vortices of figure 9 to be momentarily located on the x-axis at equal distances $R_c/2$ from the origin, as viewed from above in figure 10.
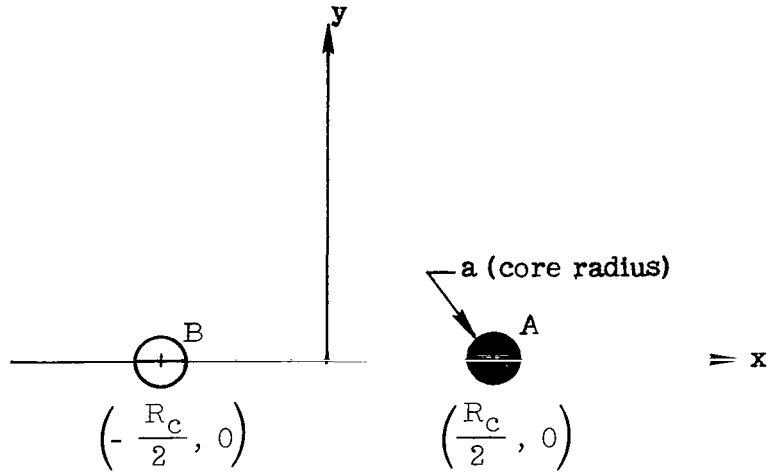


Figure 10.- View of figure 9 from above when both vertical vortices are momentarily located on the x-axis at equal distances from the origin.

Substituting equations (58) into equations (56) for the motion $\vec{U}^A$ of vortex A in the fields due to vortex B gives

$$\frac{2\pi\rho_o G}{M}\left(U_y^A - \frac{G}{R_c}\right) - \frac{K^2}{R_c^3} - \frac{G^2}{R_c^3} + \frac{U_x^B K}{R_c^2} + \frac{U_y^B G}{R_c^2} = 0 \tag{59a}$$

$$-\frac{2\pi\rho_o G}{M}\left(U_x^A - \frac{K}{R_c}\right) + \frac{U_x^B G}{R_c^2} - \frac{U_y^B K}{R_c^2} = 0 \tag{59b}$$

where the identifications $\dot{x}_m = U_x^B$ and $\dot{y}_m = U_y^B$ have been made. The symmetry of the problem dictates that $\vec{U}^B = -\vec{U}^A$. Hence, equations (59) become

$$-\frac{2\pi\rho_o G}{M}\left(U_y^A - \frac{G}{R_c}\right) + \frac{K^2}{R_c^3} + \frac{G^2}{R_c^3} + \frac{U_x^A K}{R_c^2} + \frac{U_y^A G}{R_c^2} = 0 \tag{60a}$$

$$\frac{2\pi\rho_0 G}{M}\left(U_x^A - \frac{K}{R_C}\right) + \frac{U_x^A G}{R_C^2} - \frac{U_y^A K}{R_C^2} = 0 \qquad (60b)$$

The excess mass $M$ in the partially rarefied cores is negative and may be expressed as

$$M = -\Lambda\pi a^2 \rho_0 \qquad (61)$$

where $a$ is the core radius and $\Lambda$, which has the range $0 \leqq \Lambda \leqq 1$, is a dimensionless parameter which describes the degree of rarefaction. Substituting equation (61) into equations (60) and collecting terms gives the following equations for the displacement velocity $\vec{U}^A$ of vortex A when it is located on the x-axis at a distance of $R_C$ meters from the vortex B (also on the x-axis):

$$U_y^A(1 + \beta) + U_x^A \frac{K\beta}{G} - \frac{G}{R_C} + \frac{K^2\beta}{GR_C} + \frac{G\beta}{R_C} = 0 \qquad (62a)$$

$$U_x^A(1 - \beta) + U_y^A \frac{K\beta}{G} - \frac{K}{R_C} = 0 \qquad (62b)$$

where

$$\beta = \frac{\Lambda a^2}{2R_C^2} \qquad (62c)$$

Solving these equations for $\vec{U}^A$ gives

$$\frac{U_x^A}{Q^*/2\pi R_C} = \frac{1 + \beta^2 + \dfrac{Q^{*2}\beta^2}{\Gamma^2}}{1 - \beta^2 - \dfrac{Q^{*2}\beta^2}{\Gamma^2}} \qquad (63a)$$

$$\frac{U_y^A}{\Gamma/2\pi R_C} = \frac{1 - 2\beta\left(1 + \dfrac{Q^{*2}}{\Gamma^2}\right) + \beta^2\left(1 + \dfrac{Q^{*2}}{\Gamma^2}\right)}{1 - \beta^2\left(1 + \dfrac{Q^{*2}}{\Gamma^2}\right)} \qquad (63b)$$

35

Result (63a) shows that one effect of buoyancy is to speed up the rate of approach of two vortices with convergent flow ($Q^*$ negative). It will be shown from result (63b) that another effect of buoyancy is to slow down the revolution rate of vortices of like sense.

Correlation of the twin-vortex model with data from the twin tornado.- According to results (63) for the model of twin vortices with convergence, the two vortices spiral inward toward each other, and buoyancy serves to increase the rate of approach. But instead of spiraling inward, the two funnels of the twin tornado actually increased their distance of separation from 118.9 m (390 ft) to 147.1 m (482.6 ft) according to figure 4(b). Therefore, the convergence $Q^*$ of the twin tornado may be regarded as zero, or as dominated by the boundary-layer interaction which tends to make the vortices separate. This simplified comparison, which neglects tilt, casts some doubt on the existence of significant convergence in tornadoes except within the boundary layer at the ground.

The revolution rates predicted by the present model and those observed for the twin tornado will now be compared. If $Q^{*2}/\Gamma^2$ is neglected, as seems permissible from the preceding analysis, result (63b) becomes

$$\frac{U_y^A}{\Gamma/2\pi R_c} = \frac{\left(1 - \dfrac{\Lambda a^2}{2R_c^2}\right)}{\left(1 + \dfrac{\Lambda a^2}{2R_c^2}\right)} \tag{64}$$

With both vortices momentarily located on the x-axis, equation (64) gives the ratio of the revolution rate of a buoyant vortex pair to what it would be if the vortices moved with the fluid. This expression will now be evaluated for the time when the tornado was in location 4 of figure 4, at which time both funnels appear to have had approximately equal strengths (in agreement with the assumptions of this section) according to the sketches in figure 4(c). From the photograph of the pair at location 4 in figure 5, $\dfrac{a^2}{R_c^2} \approx 0.1$ at the ground. If $\Lambda$ is taken to be 0.5, which corresponds roughly to sonic speeds at each core periphery, buoyant attraction is found to retard the revolution rate of twin vortices by about 5 percent.

According to an estimate made in appendix C, the revolution rate of the twin tornado was retarded by at least 50 percent with respect to the fluid flow. The effect of buoyant attraction, although tending in the right direction, is not sufficiently strong to account for this much retardation in the linearized theory.

The maximum possible value of $a^2/R_c^2$ for two vortices of equal core size is 1/4, which corresponds to the two vortex cores in actual contact. The retardation in this case

for $\Lambda = 0.5$ is then about 12 percent. Totally evacuated cores ($\Lambda = 1$) or cores filled with hydrogen gas ($\Lambda \approx 1$) would raise the maximum retardation to about 22 percent.

## Influence of Axial Electric Current on Revolution

## Rate of Twin Vortices

Speculative hydromagnetic-vortex hypothesis.- In this section equation (36) will be taken in the simplified form

$$\rho_0 \left\langle \vec{U} - \vec{v}^0 \right\rangle \times \vec{\Gamma} - \vec{F} = 0 \tag{65}$$

The Lorentz force term $\vec{F}$ in this equation is capable of exerting an attractive force on the funnels of the twin tornado which could retard their revolution rate to any degree, stop it altogether, or even reverse it. The possible existence of such electromagnetic forces in tornadoes is highly speculative, but it does provide an instructive application of equation (36). For a bibliography of other electrical theories concerning tornadoes, see references 16 and 17.

It is well known from electrodynamics that two parallel wires will exert an attractive force on each other if (a) they are oppositely charged or (b) they are conducting electric currents of like sense. Since the two funnels of the twin tornado were in contact with the ground, it seems unlikely that opposite static electric charges on the two funnels could be maintained. But axial electric currents of like sense could conceivably have existed in the two funnels, and this is the case that will be treated in this section.

Fluid vortices with strong axial dc electric currents are termed hydromagnetic vortices. They have been discussed by Busemann (refs. 18 and 19) for the somewhat different case of a fluid with uniformly high electrical conductivity. In the analysis to follow high conductivity is assumed to persist only in the tornado cores.

Hydromagnetic-vortex model.- Each vortex tube of the twin-tornado model (fig. 8) is characterized by coincidence of the fluid and electromagnetic states depicted in figure 11. This sketch is a view of the ground plane in the proximity of the touchdown points A and B of the tornado funnels. The broken lines represent projections in the ground plane of the tilted axes of tornadoes A and B.

Equation for vortex motion with axial electric current in a magnetic field.- The Lorentz force per unit length on an electric current filament in the presence of a magnetic field is given by

$$\vec{F} = \mu_0 \vec{I} \times \vec{H} \tag{66}$$

where $\vec{I}$ is the current in amperes, $\vec{H}$ is the magnetic field in amperes/meter, and $\mu_0$ is the magnetic permeability of vacuum in henries/meter. Substituting equation (66) into equation (65) gives

$$\rho_0 \langle \vec{U} - \vec{v}^0 \rangle \times \vec{I} + \mu_0 \langle \vec{H}^0 \rangle \times \vec{I} = 0 \tag{67}$$

where in this linearized equation, $\vec{I}$ is viewed as a perturbation current and $\vec{H}^0$ as the unperturbed magnetic field.
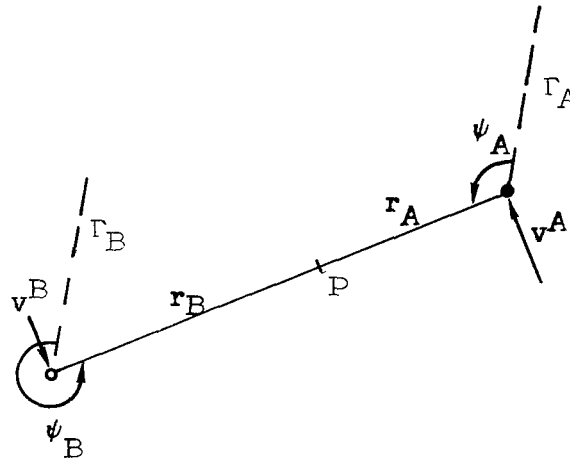


(a) Velocity fields in ground plane due to tilted vortex tubes of circulation $\Gamma^A$ and $\Gamma^B$.
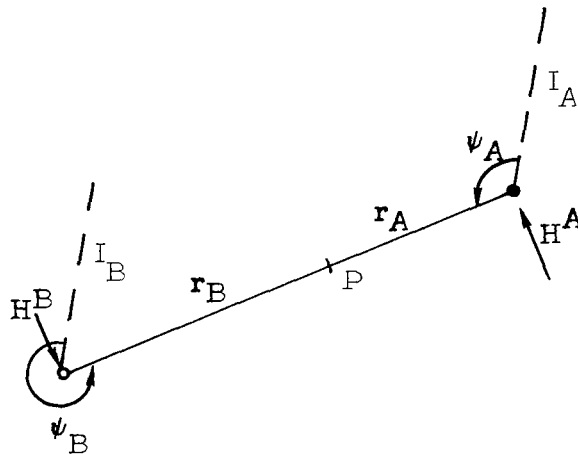


(b) Magnetic fields in ground plane due to tilted current filaments $I^A$ and $I^B$.

Figure 11.- Duplicate view from above of the ground plane, showing touchdown points of tilted hydromagnetic vortices A and B, with projections of the vortex axes indicated by broken lines.

38

As in the section entitled "Adaptation of linearized equation for vortex motion to twin-vortex model," the unperturbed fields $\vec{v}^O$ and $\vec{H}^O$ at one vortex will be those due to the other vortex. For vortex A in figure 11, equation (67) becomes

$$\rho_O\left(\vec{U}^A - \vec{v}^A\right) \times \vec{\Gamma}^A + \mu_O\vec{H}^A \times \vec{I}^A = 0 \tag{68a}$$

where the brackets have been dropped as in equations (49) and (56). And for vortex B,

$$\rho_O\left(\vec{U}^B - \vec{v}^B\right) \times \vec{\Gamma}^B + \mu_O\vec{H}^B \times \vec{I}^B = 0 \tag{68b}$$

If the cylindrical coordinate system R, $\psi$, z, with z perpendicular to the ground (see appendix A), is applied to both hydromagnetic vortices in figure 11, the radial components of equations (68) become at the ground

$$\rho_O\left(U_\psi^A - v_\psi^A\right)\Gamma_z^A + \mu_O H_\psi^A I_z^A = 0 \tag{69a}$$

$$\rho_O\left(U_\psi^B - v_\psi^B\right)\Gamma_z^B + \mu_O H_\psi^B I_z^B = 0 \tag{69b}$$

Formulas for $v_\psi$ and $H_\psi$ at the ground plane near a tilted hydromagnetic vortex are derived in appendix A. The fluid velocity fields $v_\psi^A$ and $v_\psi^B$ at the ground plane are found by applying equation (A24) of appendix A

$$v_\psi^A = \frac{\gamma_B}{2\pi R_c} \tag{70a}$$

where $R_c$ is the center-to-center distance in the ground plane and

$$\gamma_B = \frac{\Gamma_B}{D}\left(1 - \sin\chi\cos\psi_A\right) \tag{70b}$$

$$D \equiv \sqrt{1 - \sin^2\chi\cos^2\psi_A}\sqrt{1 + \tan^2\chi\sin^2\psi_A} \tag{70c}$$

Also,

$$v_\psi^B = \frac{\gamma_A}{2\pi R_c} \tag{70d}$$

$$\gamma_A = \frac{\Gamma_A}{D}\left(1 + \sin\chi\cos\psi_A\right) \tag{70e}$$

The magnetic fields $H_\psi^A$ and $H_\psi^B$ are obtained from equation (A23):

$$H_\psi^A = \frac{i_B}{2\pi R_c} \tag{71a}$$

where

$$i_B = \frac{I_B}{D}\left(1 - \sin\chi\cos\psi_A\right) \tag{71b}$$

and

$$H_\psi^B = \frac{i_A}{2\pi R_c} \tag{71c}$$

where

$$i_A = \frac{I_A}{D}\left(1 + \sin\chi\cos\psi_A\right) \tag{71d}$$

Expressions (70) and (71) will be used as mean values for the velocity and magnetic fields over the vortex cross sections.

The vortex end points A and B are assumed to revolve about the point P (fig. 11) defined by the equations

$$\gamma_A r_A = \gamma_B r_B \tag{72}$$

$$r_A + r_B = R_c \tag{73}$$

with displacement velocities

$$U_\psi^A = r_A \dot{\psi}_A(I) \tag{74a}$$

and

$$U_\psi^B = r_B \dot{\psi}_B(I) \tag{74b}$$

where the revolution rate $\dot{\psi}_A(I) = \dot{\psi}_B(I)$ is now a function of the axial electric currents in the vortex cores. Equation (72) may also be written, by use of equation (73),

$$\frac{\gamma_B}{r_A} = \frac{\gamma_A + \gamma_B}{R_c} \tag{75}$$

40

Solution for revolution rate of inclined hydromagnetic vortex pair at the ground.-
Substituting equations (70), (71), and (73) in equations (69) and noting that $\Gamma_z = \Gamma \cos \chi$
and $I_z = I \cos \chi$ for both touchdown points (see appendix A) gives at A

$$\rho_0 \Gamma_A \left[ \frac{\gamma_B}{2\pi R_c} - r_A \dot{\psi}_A(I) \right] = \frac{\mu_0 I_A{}^i{}_B}{2\pi R_c} \tag{76a}$$

and at B

$$\rho_0 \Gamma_B \left[ \frac{\gamma_A}{2\pi R_c} - r_B \dot{\psi}_B(I) \right] = \frac{\mu_0 I_B{}^i{}_A}{2\pi R_c} \tag{76b}$$

If equation (76a) is multiplied by the factor $\left( 1 + \sin \chi \cos \psi_A \right)/D$ and equation (76b)
by the factor $\left( 1 - \sin \chi \cos \psi_A \right)/D$, equations (76) become upon substitution of equations (70b), (70e), (71b), and (71d)

$$\rho_0 \gamma_A \left[ \frac{\gamma_B}{2\pi R_c} - r_A \dot{\psi}_A(I) \right] = \frac{\mu_0 i_A{}^i{}_B}{2\pi R_c} \tag{77a}$$

and

$$\rho_0 \gamma_B \left[ \frac{\gamma_A}{2\pi R_c} - r_B \dot{\psi}_B(I) \right] = \frac{\mu_0 i_A{}^i{}_B}{2\pi R_c} \tag{77b}$$

Equating the left-hand sides of equations (77a) and (77b) and collecting terms gives

$$\gamma_A r_A \dot{\psi}_A(I) = \gamma_B r_B \dot{\psi}_B(I) \tag{78}$$

Relation (72) then shows that

$$\dot{\psi}_B(I) = \dot{\psi}_A(I) \tag{79}$$

which verifies that point P is the center point of revolution of points A and B in the
ground plane, as assumed for equations (74).

If equation (77a) is multiplied by $2\pi R_c$ and equation (75) is substituted, then

$$\rho_0 \gamma_A \gamma_B \left[ 1 - \frac{2\pi R_c^2 \dot{\psi}_A(I)}{\gamma_A + \gamma_B} \right] = \mu_0 i_A{}^i{}_B \tag{80}$$

But $\dfrac{\gamma_A + \gamma_B}{2\pi R_c^2}$ is the revolution rate $\dot{\psi}_A$ of touchdown points A and B in the absence of

axial electric currents, and equation (80) may be written

$$\rho_0 \gamma_A \gamma_B \left[1 - \frac{\dot{\psi}_A(I)}{\dot{\psi}_A}\right] = \mu_0 i_A i_B \tag{81}$$

where $\dot{\psi}_A(I)$ denotes the revolution rate of points A and B with axial electric currents, and $\dot{\psi}_A$ the revolution rate without electric currents. Substitution of definitions (70b), (70e), (71b), and (71d) also gives

$$\rho_0 \Gamma_A \Gamma_B \left[1 - \frac{\dot{\psi}_A(I)}{\dot{\psi}_A}\right] = \mu_0 I_A I_B \tag{82}$$

Now take the axial electric current for each funnel to be proportional to its individual circulation

$$\left. \begin{array}{l} I_A = \kappa \Gamma_A \\[2em] I_B = \kappa \Gamma_B \end{array} \right\} \tag{83}$$

Substitution of these relations in equation (82) results in the following equation for $\kappa$, in A-sec/m$^2$,

$$\kappa = \sqrt{\frac{\rho_0}{\mu_0}\left[1 - \frac{\dot{\psi}_A(I)}{\dot{\psi}_A}\right]} \tag{84}$$

<u>Order of magnitude of axial electric current which would account for retarded revolution rate of twin tornado.</u>- In appendix C it is estimated that the revolution rate of the twin funnels was retarded by at least one-half with respect to the fluid flow and that the actual circulation of the pair $\Gamma_A + \Gamma_B$ was probably greater than $10^4$ m$^2$/sec. Substituting the values

$$\Gamma_A + \Gamma_B = 10^4 \text{ m}^2/\text{sec} \tag{85a}$$

$$\rho_0 = 1.18 \text{ kg/m}^3 \tag{85b}$$

$$\mu_0 = 4\pi \times 10^{-7} \text{ H/m} \tag{85c}$$

$$\frac{\dot{\psi}_A(\text{I})}{\dot{\psi}_A} = \frac{1}{2} \tag{85d}$$

in equation (84) gives for air near sea level

$$\kappa = 6.86 \times 10^2 \text{ amp-sec/m}^2 \tag{86}$$

and by equations (83) the total axial electric current which would be required to slow down the free revolution rate of the twin tornado to one-half that of the fluid flow is

$$I_A + I_B = 6.86 \times 10^6 \text{ A} \tag{87}$$

It was estimated in the section entitled "Effect of Core Buoyancy on Revolution Rate of a Twin Tornado" that buoyant attraction could have reduced the revolution rate of the twin tornado by about 5 percent. To accomplish the same 5-percent reduction by magnetic attraction would require a total axial electric current of $2.16 \times 10^6$ amperes in the funnels. This would make the total magnetic energy of a tornado $\iiint \frac{\mu_0 H^2}{2} dV$ comparable in magnitude with its kinetic energy $\iiint \frac{\rho_0 v^2}{2} dV$. Such electric currents are much larger than values previously proposed as possibly existent in tornadoes (refs. 20 to 24).

## CONCLUDING REMARKS

The new equation for the motion of vorticity derived in this paper is found to have application to the motion of tornadoes and tornado cyclones. Quantitatively, the most successful of these applications of the equation in its linearized form appears to be the explanation given for the tendency of severe local storms (tornado cyclones) to move to the right of the mean tropospheric wind by virtue of their interaction with the jet stream. Also successful was finding that the effect of the boundary layer at the ground on the twin tornado of April 11, 1965, near Elkhart, Indiana, was to make the two funnels separate, as they were observed to do. The increasing separation of the twin tornado also appears to constitute evidence against the possibility of convergent flow in the funnels of the twin tornado except within the boundary layer at the ground.

Less successful, quantitatively, were attempts at explaining why the funnels of the twin tornado apparently revolved about each other at a much slower rate than the fluid flow. The retardation in revolution rate was estimated to be about 50 percent with respect to the fluid. Two mechanisms were found which could retard the revolution rate: (1) buoyant attraction of each partially rarefied tornado core in the radial pressure gradient of the other core, and (2) magnetostatic attraction between axial dc electric currents of like sense in the cores. The retardation due to buoyant attraction was calculated to be about 5 percent for the twin tornado. In general buoyant attraction could retard the revolution rate of hollow-core or helium-core vortices of like sense by as much as 22 percent. Retardation by magnetostatic attraction requires electric currents in the tornado cores which are much larger than existing evidence would indicate.

A potentially important buoyancy effect was not included in this report, that is the upward lift on buoyant atmospheric vortices which are tilted with respect to the vertical. The most significant new result appears to be the equation for vortex motion, itself. Since it is free of constraints on the fluid medium or on the flow or force fields, it should find applications in meteorology concerning the motions of various cyclones.

Langley Research Center,
National Aeronautics and Space Administration,
Hampton, Va., July 24, 1970.

# APPENDIX A

## DERIVATION OF MAGNETIC AND VELOCITY FIELDS AT THE GROUND
## PLANE NEAR A TILTED HYDROMAGNETIC VORTEX

Determining the velocity field due to a tilted vortex above the ground is identical with the problem of determining the magnetic field due to an electric current in a tilted wire above the ground when it is specified that the magnetic field does not penetrate the ground. This is assured by making the ground plane a perfect electrical conductor, as shown in figure 12(a). Of these two analogs, the electrical lends itself simply to solution
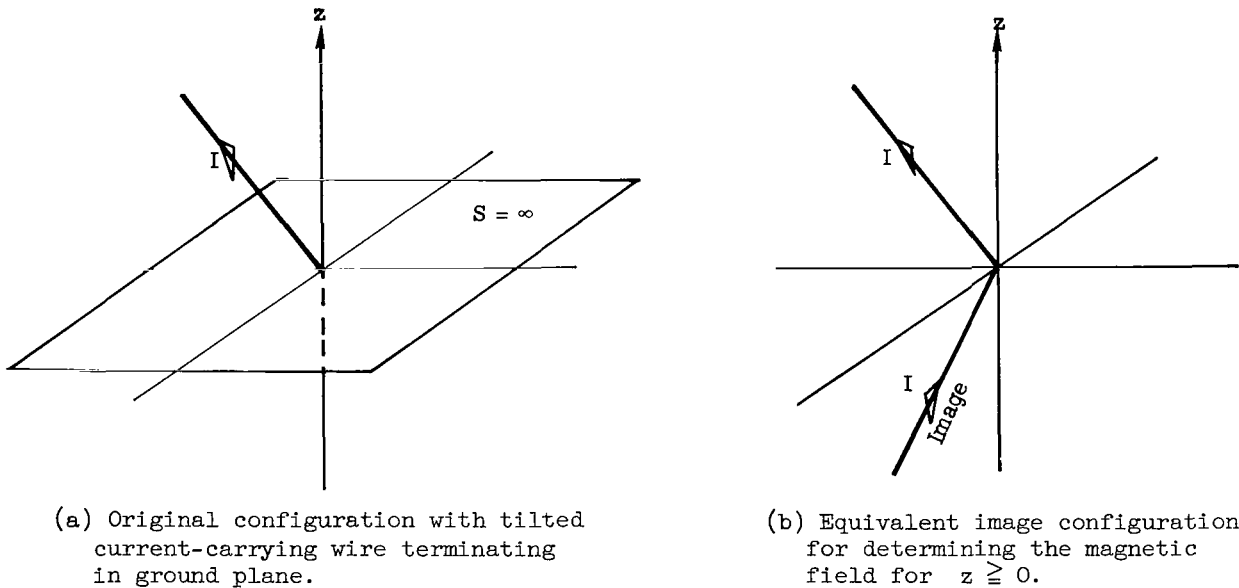


(a) Original configuration with tilted current-carrying wire terminating in ground plane.

(b) Equivalent image configuration for determining the magnetic field for $z \geq 0$.

Figure 12.- Image method for magnetic fields due to steady electric current $I$ in tilted wire above perfectly conducting ground plane.

by the method of images because $\text{div } \vec{J} = -\dfrac{\partial \rho_e}{\partial t}$, whereas $\text{div } \vec{\omega} = 0$. This distinction means that a vortex line cannot terminate at an interior point of the flow field, while an electric-current filament can terminate (by allowing accumulation of charge at the termination point) and this is what is needed in the method of images. Therefore, the electric-current—magnetic-field problem will be solved initially by the method of images, and the circulation—velocity-field solutions will be determined afterward by analogy.

In the image method the perfectly conducting ground plane of figure 12(a) is replaced by the image of the wire, as depicted in figure 12(b). The magnetic-field

solution for this sharply bent wire is then obtained by superposition of the magnetic-field solutions for the two straight semi-infinite wire sections. The first concern, therefore, is to determine the magnetic field about a straight semi-infinite wire bearing a uniform current I, as illustrated in figure 13.
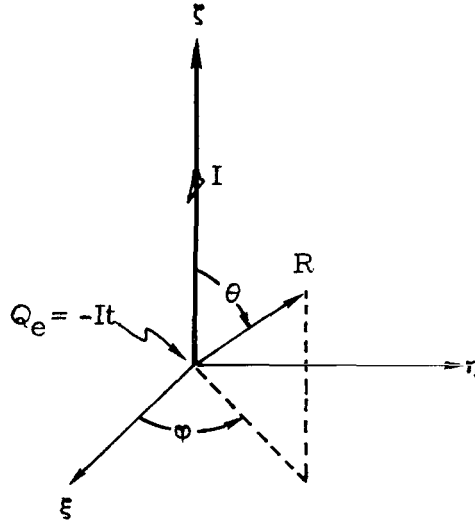
Figure 13.- Semi-infinite wire in spherical coordinate system, showing uniform direct current $\vec{I}$ along the $\zeta$-axis and charge accumulation $Q_e$ at the origin.

A suitable representation for the current density $J_\zeta$ in the wire is given by

$$J_\zeta = I\delta(\xi)\delta(\eta)H(\zeta) \tag{A1}$$

where $\delta$ is the Dirac delta function and $H(\zeta)$ is the Heaviside unit step function. The continuity equation for current and charge densities

$$\frac{\partial J_\zeta}{\partial \zeta} + \frac{\partial \rho_e}{\partial t} = 0 \tag{A2}$$

requires a buildup of negative charge density $\rho_e$ at the termination point of the wire, as represented by the expression

$$\rho_e = -It\delta(\xi)\delta(\eta)\delta(\zeta) \tag{A3}$$

(This negative charge will be canceled out upon superposition by an equivalent positive charge at the end of the image wire.) Maxwell's equations in a medium with negligible electric and magnetic polarization are

46

$$\text{curl } \vec{H} = \epsilon_0 \dot{\vec{E}} + \vec{J} \tag{A4a}$$

$$\text{div } \epsilon_0 \vec{E} = \rho_e \tag{A4b}$$

$$\text{curl } \vec{E} = 0 \tag{A4c}$$

$$\text{div } \vec{H} = 0 \tag{A4d}$$

where $\dot{\vec{H}}$ has been equated to zero because the free current density $\vec{J} = \hat{\zeta} J_\zeta$ and the displacement current density $\epsilon_0 \dot{\vec{E}}$ are constants.

It is apparent from the geometry in figure 13 and from equations (A4b) and (A4c) that the electric field $\vec{E}$ is purely radial, is spherically symmetric, and is given by

$$\vec{E} = \hat{R} E_R$$

where

$$E_R = -\frac{It}{4\pi\epsilon_0 R^2} \tag{A5}$$

Hence,

$$\dot{E}_R = -\frac{I}{4\pi\epsilon_0 R^2} \tag{A6}$$

The integral form of equation (A4a) on a spherical surface $S$ of radius $R$ is

$$\oint \vec{H} \cdot d\vec{l} = \iint \left( \epsilon_0 \dot{\vec{E}} + \vec{J} \right) \cdot \hat{R} \, dS \tag{A7}$$

If the closed contour line $l$ is taken to be a circle perpendicular to the wire and if the area of integration $S$ is that portion of the spherical surface enclosed by $l$, as depicted in figure 14, equation (A7) becomes

$$2\pi R H_\varphi \sin \theta = I + \int_0^\theta 2\pi\epsilon_0 R^2 \dot{E}_R \sin \Theta \, d\Theta \tag{A8}$$

Integrating the last term of equation (A8) and collecting terms gives for the axisymmetric azimuthal magnetic field

$$H_\varphi = \frac{I}{4\pi R} \frac{(1 + \cos \theta)}{\sin \theta} \tag{A9}$$
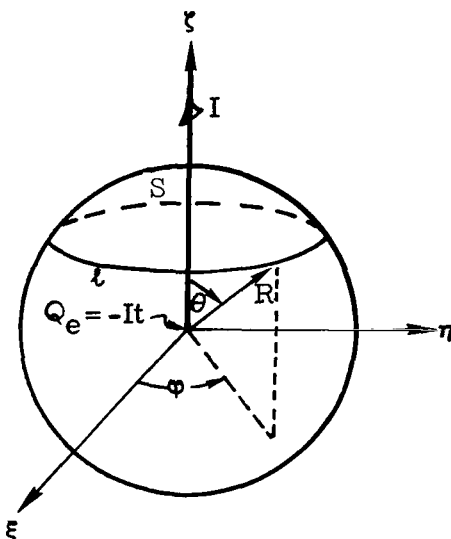
Figure 14.- Surface of integration  S  for equation (A7)
and its bounding circuit line  $l$  on the spherical
surface  R = Constant  in the coordinate system  R,θ,φ.

Now take the straight semi-infinite wire to lie in the xz-plane of a Cartesian coordinate system, inclined at an angle  $\chi$  to the z-axis, as pictured in figure 15.  The radius vector  $\vec{R}$  will now be confined to the xy-plane.  The amplitude of the magnetic field  $H_{\varphi}$  (eq. (A9)) at all points in the xy-plane (or Rψ-plane) will now be determined. All that is necessary is to evaluate  $\cos\theta$  and  $\sin\theta$  of equation (A9) in terms of the angles  $\chi$  and  $\psi$.

The formula for  $\cos\theta$  from analytic geometry is

$$\cos\theta = \lambda_I\lambda_R + \mu_I\mu_R + \nu_I\nu_R \tag{A10}$$

where the direction cosines  $\lambda_I,\mu_I,\nu_I$  of  $\vec{I}$  and  $\lambda_R,\mu_R,\nu_R$  of line  $\vec{R}$  are given by

$$\left.\begin{aligned}\lambda_I &= \sin\chi \\ \mu_I &= 0 \\ \nu_I &= \cos\chi\end{aligned}\right\} \tag{A11}$$

and

$$\left.\begin{aligned}\lambda_R &= \cos\psi \\ \mu_R &= \sin\psi \\ \nu_R &= 0\end{aligned}\right\} \tag{A12}$$
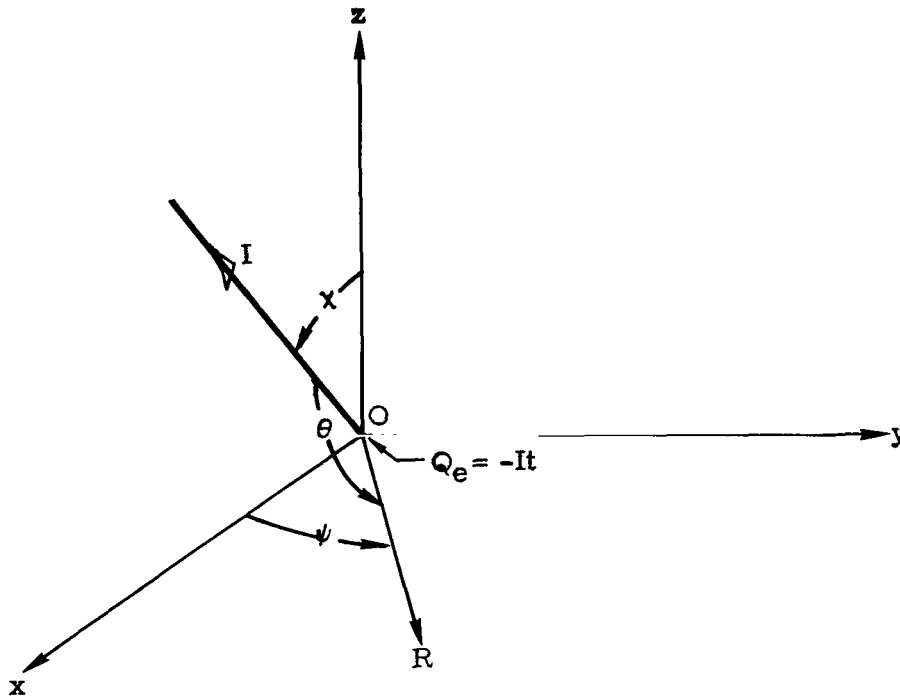
48

Figure 15.- Configuration of figure 13 tilted and embedded in a Cartesian coordinate system x,y,z. The current-carrying wire is taken to lie in the xz-plane and the radius vector R in the xy-plane.

Thus,

$$\cos \theta = \sin \chi \cos \psi \tag{A13}$$

and

$$\sin \theta = \sqrt{1 - \sin^2\chi \cos^2\psi} \tag{A14}$$

and the magnitude of the magnetic field at points in the xy-plane is given by

$$H_\varphi = \frac{I}{4\pi R} \frac{(1 + \sin \chi \cos \psi)}{\sqrt{1 - \sin^2\chi \cos^2\psi}} \qquad (z = 0) \tag{A15}$$

This magnetic field is oriented in the direction of $\vec{\tau}$ where $\vec{\tau}$ is normal to the plane formed by the vectors $\vec{I}$ and $\vec{R}$, as shown in figure 16.
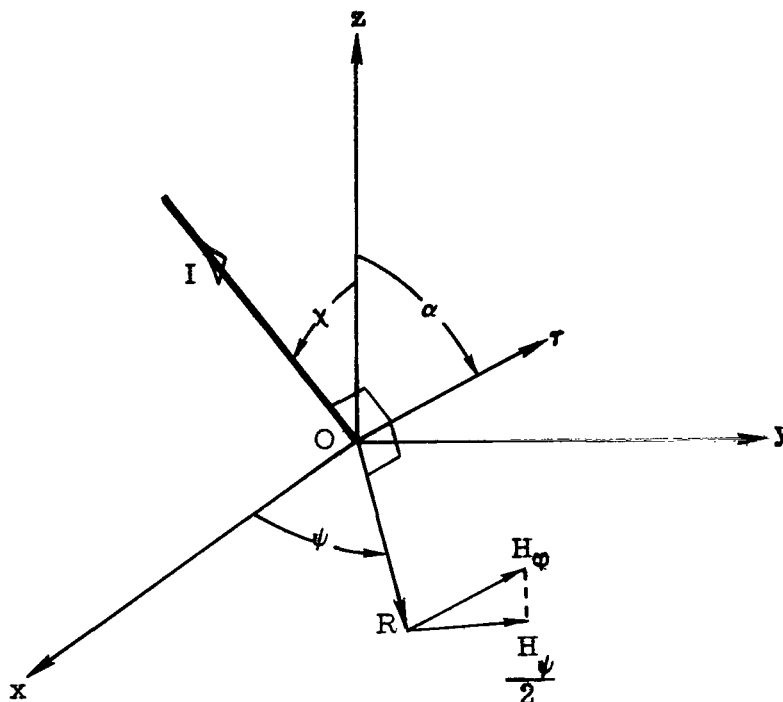
Figure 16.- Direction $\vec{\tau}$ of magnetic field $H_\varphi$ at $z = 0$
due to a semi-infinite tilted current-carrying wire.
The horizontal component, denoted $H_\psi/2$, is also shown.

If $\lambda, \mu, \nu$ are the direction cosines of $\vec{\tau}$, the condition that $\vec{\tau}$ be perpendicular to both $\vec{I}$ and $\vec{R}$ is expressed by

$$\lambda_I \lambda + \nu_I \nu = 0 \qquad\qquad \text{(A16a)}$$

$$\lambda_R \lambda + \mu_R \mu = 0 \qquad\qquad \text{(A16b)}$$

$$\lambda^2 + \mu^2 + \nu^2 = 1 \qquad\qquad \text{(A16c)}$$

where the fact that $\mu_I = \nu_R = 0$ has been used. Substituting $\nu$ from equation (A16a) and $\mu$ from equation (A16b) into equation (A16c) and solving for $\lambda^2$ gives

$$\lambda^2 = \left(1 + \frac{\lambda_I^2}{\nu_I^2} + \frac{\lambda_R^2}{\mu_R^2}\right)^{-1} \qquad\qquad \text{(A17)}$$

or from equations (A11) and (A12),

$$\lambda^2 = \left(\csc^2\psi + \tan^2\chi\right)^{-1} \qquad\qquad \text{(A18)}$$

50

In figures 12 and 16, the z-component of $H_\varphi$ at points on the xy-plane will be nullified by the z-component of the image wire. But the horizontal component, which is proportional to $\sin \alpha$, will be doubled by the image field on the xy-plane. Therefore, the total magnetic field in the ground plane xy due to current in a straight tilted wire above the ground plane is horizontal, purely azimuthal, and given by

$$H_\psi = 2H_\varphi \sin \alpha \qquad (z = 0) \qquad\qquad \text{(A19)}$$

In terms of the direction cosines of $\vec{\tau}$,

$$\sin^2\alpha = 1 - \nu^2 = \lambda^2 + \mu^2 \qquad\qquad \text{(A20)}$$

and from equation (A16b)

$$\sin^2\alpha = \lambda^2\left(1 + \frac{\lambda_R^2}{\mu_R^2}\right) \qquad\qquad \text{(A21)}$$

Substituting equations (A12) and (A18) gives after some reduction

$$\sin \alpha = \left(1 + \sin^2\psi \tan^2\chi\right)^{-1/2} \qquad\qquad \text{(A22)}$$

Substitution of equations (A15) and (A22) in relation (A19) gives for the magnetic field $H_\psi$ in the ground plane due to current $I$ in a straight tilted wire above the ground plane

$$H_\psi = \frac{I}{2\pi R} \frac{1 + \sin \chi \cos \psi}{\sqrt{1 - \sin^2\chi \cos^2\psi}\sqrt{1 + \tan^2\chi \sin^2\psi}} \qquad (z = 0) \qquad \text{(A23)}$$

where the coordinates $R$ and $\psi$ in the ground plane and the tilt angle $\chi$ are shown in figure 17.
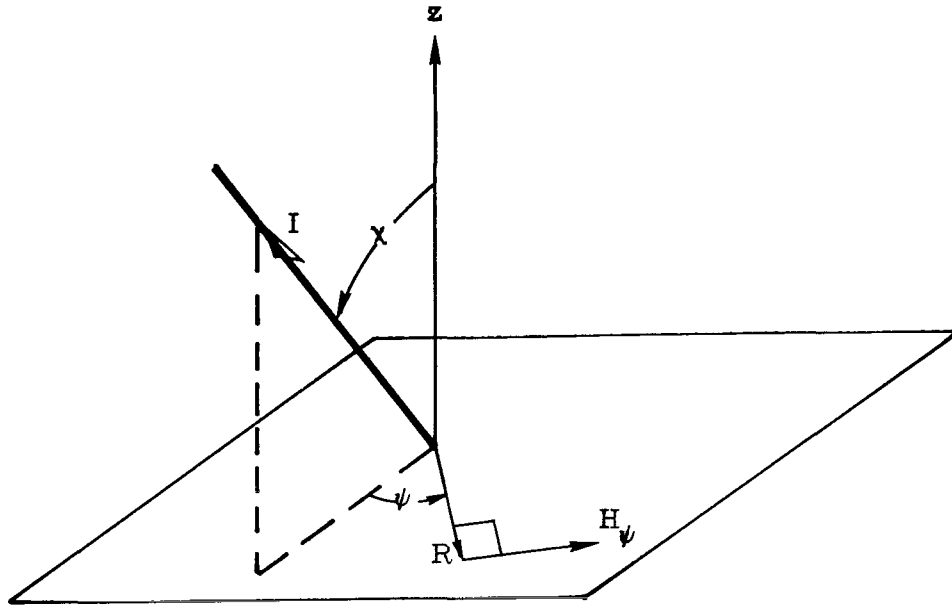
Figure 17.- Coordinate system for equation (A23).

Since $\vec{I}$ and $\vec{H}$ in electrodynamics are analogous to $\vec{\Gamma}$ and $\vec{v}$ in fluid dynamics,

$$v_\psi = \frac{\Gamma}{2\pi R} \frac{1 + \sin\chi\cos\psi}{\sqrt{1 - \sin^2\chi\cos^2\psi}\sqrt{1 + \tan^2\chi\sin^2\psi}} \qquad (z = 0) \qquad \text{(A24)}$$

where $v_\psi$ is the velocity field in the ground plane due to a straight tilted vortex of circulation $\Gamma$ above the ground plane. The vortex configuration for equation (A24) is shown in figure 18.
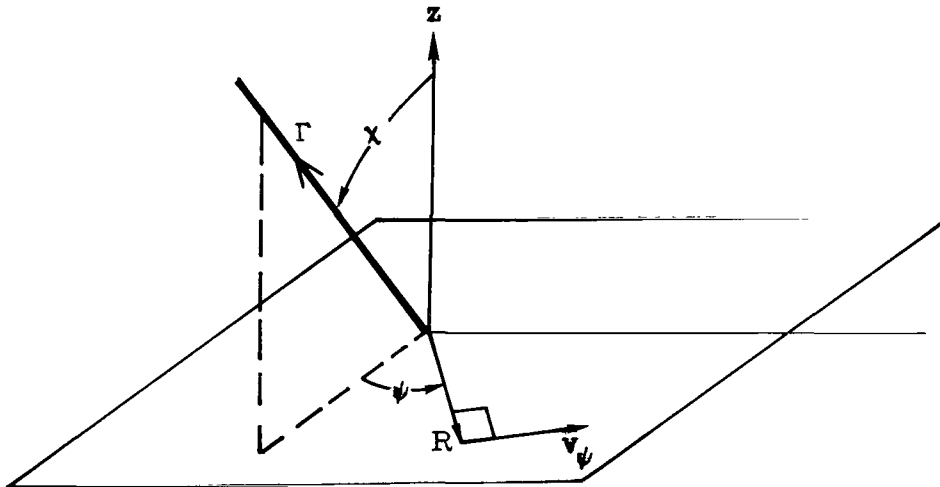


Figure 18.- Coordinate system for equation (A24).

# APPENDIX B

## DESCRIPTION AND TABULATION OF EMPIRICAL DATA

## ON TWIN TORNADO OF APRIL 11, 1965,

## NEAR ELKHART, INDIANA

An unusual tornado, identified J-2 in reference 4, occurred on April 11, 1965, near Elkhart, Indiana. This tornado developed a second funnel, and the two funnels revolved about each other for about 1 minute, and then the original funnel disappeared. Six photographs of the tornado were taken during the period of duality by Paul Huffman of the Elkhart Truth. One of these photographs is reproduced in figure 5. On the basis of these photographs and aerial examination of the damage paths, Fujita determined that the circulation of both funnels during their brief period of individuality was cyclonic, and he produced figure 4 (fig. 49 in ref. 4) which shows to scale the motion of the two vortices. The time intervals between the photographs were determined from the translational speed of the storm, about 22.4 m/sec (50 mph).

From a fourfold enlargement of figure 4(b), the following parameters have been obtained for each of the locations 3 to 6: (1) the center-to-center distance $R_c$ of the twin vortices; (2) the tilt angle $\chi$ of the pair with respect to the vertical; and (3) the azimuth angle $\psi_A$ of the pair in the ground plane. These quantities are listed in table I. The azimuth angle $\psi_A$ is the angle at funnel A measured counterclockwise from the broken line labeled "tilt 29°" in figure 4(b) to the line $AB$ connecting the centers of the vortex pair. The diameters of the spots in figure 4(c) were taken to be indicative of their relative strengths and were used to calculate the tabulated values for the ratio $\Gamma_B/\Gamma_A$.

For each of the three intervals between these four data points interpolation gives the mean separation $\langle R_c \rangle$, the mean tilt angle $\langle \chi \rangle$, the mean azimuth angle $\langle \psi_A \rangle$, the mean revolution rate $\langle \dot{\psi}_A \rangle$, and the mean circulation ratio $\langle \Gamma_B/\Gamma_A \rangle$. These quantities are listed in table II. Also included for use in appendix C are mean values

$\langle D \rangle$ where $D \equiv \sqrt{1 - \sin^2\chi \cos^2\psi_A} \sqrt{1 + \tan^2\chi \sin^2\psi_A}$.

# APPENDIX C

## CIRCULATION OF THE TWIN TORNADO AS DEDUCED

## FROM ITS REVOLUTION RATE –

## EVIDENCE THAT THE FUNNELS MOVED MORE SLOWLY THAN THE FLUID

### Circulation Estimate From Revolution Rate

In this appendix the total circulation $\Gamma_A + \Gamma_B$ of the twin tornado will first be estimated from its revolution rate with the assumption that the funnels move with the fluid. According to equation (36) this means that the buoyancy and source terms are neglected as well as a possible Lorentz force $\vec{F}$. The effects of these terms have been determined, subject to certain simplifications, in the sections entitled, "Effect of Core Buoyancy on Revolution Rate of a Twin Tornado," "Effect of the Boundary Layer at the Ground on Tornado Motion," and "Influence of Axial Electric Current on Revolution Rate of Twin Vortices." After the first estimate is obtained, the effects of the neglected terms on this estimate will be considered.

The velocity fields are determined in accordance with the twin-vortex model presented in the section entitled, "Tornado model" and illustrated in figure 8. Effects of the tilt angle $\chi$ and of the unequal circulations $\Gamma_A$ and $\Gamma_B$ of the two vortices are included. But the convergences $Q_A^*$ and $Q_B^*$ of this model are equated to zero in order to conform to the observation that the twin funnels did not approach each other, as explained in the section entitled, "Correlation of the twin-vortex model with data from the twin tornado."

Velocity field at ground plane due to single inclined vortex.- Consider a single vortex of circulation $\Gamma$ which terminated on the ground plane and is inclined to the vertical by the angle $\chi$ as in figure 18. The velocity field at the ground plane ($R\psi$-plane) for such a vortex in a perfect fluid is found in appendix A (eq. (A24)) to be purely azimuthal and given by the formula

$$v_\psi(R,\psi) = \frac{\Gamma}{2\pi R} \frac{1 + \sin\chi\cos\psi}{\sqrt{1 - \sin^2\chi\cos^2\psi}\sqrt{1 + \tan^2\chi\sin^2\psi}} \qquad (z = 0)$$

Twin-vortex model.- Now, consider the configuration shown in figure 8 as viewed from above in figure 19. Here the two tilted, semi-infinite vortices terminate at spots A and B in the ground plane. The broken lines in this figure represent the projections of the vortex axes in the ground plane, as in figure 4(b). Take the two inclined vortices to be parallel to each other and to have cyclonic circulations $\Gamma_A$ and $\Gamma_B$ in a perfect
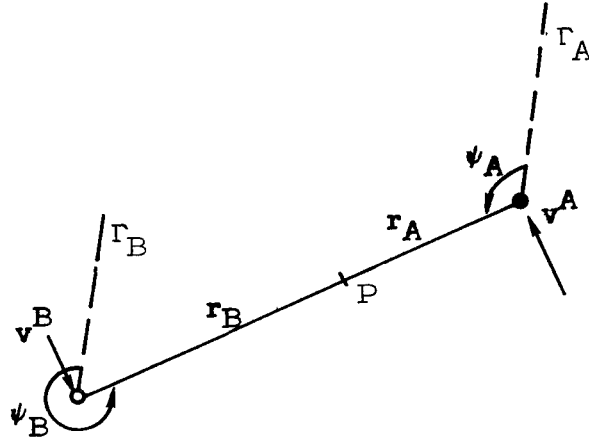
Figure 19.- View of ground plane from above (as in fig. 4(b))
showing the touchdown points of two vortices A and B, their
velocity fields, and orientation with respect to projections
of the vortex axes.

fluid which is otherwise at rest. The velocity field $\vec{v}^B$ at point B is perpendicular to the line AB, as shown in figure 19, and is given by

$$v_\psi^B = \frac{\gamma_A}{2\pi R_c} \tag{C1}$$

where

$$\gamma_A = \frac{\Gamma_A}{D}\left(1 + \sin \chi \cos \psi_A\right) \tag{C2}$$

and

$$D \equiv \sqrt{1 - \sin^2\chi \cos^2\psi_A}\sqrt{1 + \tan^2\chi \sin^2\psi_A} \tag{C3}$$

Similarly, the velocity field $\vec{v}^A$ is given by

$$v_\psi^A = \frac{\gamma_B}{2\pi R_c} \tag{C4}$$

where

$$\gamma_B = \frac{\Gamma_B}{D}\left(1 - \sin \chi \cos \psi_A\right) \tag{C5}$$

55

and the substitution $\psi_B = \psi_A \pm \pi$ has been made. The quantities $\gamma_A$ and $\gamma_B$ will be referred to as the "effective circulations" of vortices A and B.

Define point P on the line AB, as shown in figure 19 so that

$$\gamma_A r_A = \gamma_B r_B \tag{C6a}$$

$$r_A + r_B = R_c \tag{C6b}$$

Then the revolution rates of points A and B about P are given by

$$\dot{\psi}_A = \frac{v_\psi^A}{r_A} = \frac{\gamma_B}{2\pi R_c r_A} \tag{C7}$$

$$\dot{\psi}_B = \frac{v_\psi^B}{r_B} = \frac{\gamma_A}{2\pi R_c r_B} \tag{C8}$$

But by relation (C6a)

$$\dot{\psi}_B = \dot{\psi}_A \tag{C9}$$

and point P is seen to be the center point of revolution of points A and B in the ground plane. $\left(\text{Since } \gamma_A \text{ and } \gamma_B \text{ are different functions of } \psi_A, \text{ the location of point P on line AB will also vary with the azimuth angle } \psi_A \text{ of the pair.}\right)$ Combination of equations (C6a) and (C6b) gives

$$\frac{\gamma_B}{r_A} = \frac{\gamma_A + \gamma_B}{R_c} \tag{C10}$$

Hence, the theoretical revolution rate in the ground plane of a tilted vortex pair of like sense in a perfect fluid is given by

$$\dot{\psi}_A = \frac{\gamma_A + \gamma_B}{2\pi R_c^2} \tag{C11}$$

The effective circulation $\gamma_A + \gamma_B$ of the vortex pair is related to the circulation $\Gamma_A + \Gamma_B$ by adding equations (C2) and (C5)

$$\gamma_A + \gamma_B = \frac{\Gamma_A + \Gamma_B}{D} - \frac{\Gamma_B - \Gamma_A}{D} \sin \chi \cos \psi_A \tag{C12}$$

where $D$ is given by equation (C3). Combining equations (C11) and (C12) gives

$$2\pi R_c^2 D \dot{\psi}_A = \Gamma_A (1 + b) + \Gamma_A (1 - b) \sin \chi \cos \psi_A \tag{C13}$$

where $b \equiv \Gamma_B / \Gamma_A$. Solving for $\Gamma_A$:

$$\Gamma_A = \frac{2\pi R_c^2 D \dot{\psi}_A}{(1 + b) + (1 - b) \sin \chi \cos \psi_A} \tag{C14}$$

and multiplying by $(1 + b)$ gives

$$\Gamma_A + \Gamma_B = \frac{2\pi R_c^2 D \dot{\psi}_A (1 + b)}{(1 + b) + (1 - b) \sin \chi \cos \psi_A} \tag{C15}$$

For intervals 3-4, 4-5, and 5-6 mean values $\langle \Gamma_A + \Gamma_B \rangle$ can be determined by substituting values from table II for $\langle R_c \rangle$, $\langle D \rangle$, $\langle \psi_A \rangle$, $\langle b \rangle$, $\langle \chi \rangle$, and $\langle \dot{\psi}_A \rangle$ in formula (C15). This gives the following estimate for $\langle \Gamma_A + \Gamma_B \rangle$ in $m^2/sec$:

$$\langle \Gamma_A + \Gamma_B \rangle = \begin{cases} 5.51 \times 10^3 & \text{(Interval 3-4)} \\ 4.34 \times 10^3 & \text{(Interval 4-5)} \\ 4.91 \times 10^3 & \text{(Interval 5-6)} \end{cases} \tag{C16}$$

Averaging these values gives

$$\langle \Gamma_A + \Gamma_B \rangle = 4.92 \times 10^3 \quad \text{(interval 3-6)} \tag{C17}$$

for the total circulation in $m^2/sec$ of the tornado pair, as computed from the revolution rate of their touchdown spots on the ground with the assumption that the funnels move with the fluid.

## Evidence That the Revolution Rate Was Retarded

## With Respect to the Fluid

Examining the wind damage shown in figure 20 shows that the value (C17) for $\langle \Gamma_A + \Gamma_B \rangle$ is too small by at least a factor of 2.  This photograph views the Midway Trailer Court from the north.  This trailer court was hit by the twin tornado.  The two funnels moved from right to left across this photograph and were tilted toward the bottom edge of the photograph.  Figure 5, which depicts the funnels at location 4, was taken while funnel B was over the trailer court.



UPTURNED TRAILER

Figure 20.- Aerial photograph of severe damage to the Midway Trailer Court near Elkhart, Indiana.  Devastation seen near center of picture was caused by the left funnel of the tornado shown in figure 5, while the right funnel moved over the plowed field from right to left, cutting across upper corner of the court.  Damage occurred at 5:32 p.m. CST, April 11, 1965; picture was taken April 13.  Courtesy T. Fujita (ref. 4).

Note the damage near the lower edge of figure 20 left of center.  One trailer has a side blown out, and next to it is one which was upturned (wheels up).  The maximum possible wind speed at this point due to the calculated value (C17) for $\langle \Gamma_A + \Gamma_B \rangle$ can be determined by combining the two funnels into a single vortex on the nearest tornado path and tilting this vortex directly toward the upturned trailer.  The center of the nearest

path is a distance of 89.9 m (295 ft) from the upturned trailer. (This distance estimate assumes that the trailers were typically 15.2 m (50 ft) long.) The nearest path is that of funnel B, which cut diagonally from upper right to center left across the trailer court and caused the devastation near the middle of the photograph.

The velocity field at the ground due to a single tilted vortex (fig. 18) is given by equation (A24). Substituting the values

$$\left.\begin{aligned}
\Gamma &= \left\langle \Gamma_A + \Gamma_B \right\rangle = 4.92 \times 10^3 \ \mathrm{m^2/sec} \\
R &= 89.9 \ \mathrm{m} \ \ (295 \ \mathrm{ft}) \\
\chi &= 29^{\mathrm{o}} \\
\psi_A &= 0^{\mathrm{o}}
\end{aligned}\right\} \tag{C18}$$

in equation (A24) gives

$$v_\psi = 14.8 \ \mathrm{m/sec} \ \ (33.1 \ \mathrm{mph}) \tag{C19}$$

as the maximum possible wind speed at the upturned trailer due to the circulation value $\left\langle \Gamma_A + \Gamma_B \right\rangle = 4.92 \times 10^3 \ \mathrm{m^2/sec}$ calculated from the revolution rate of the pair, assumed to move with the fluid. This wind speed is clearly too low, and it is not augmented by the speed of the storm, about 22.4 m/sec (50 mph), because the site of the upturned trailer was on the northern side of the tornado path, where the storm velocity opposes and tends to reduce the circulation velocity. In reference 3, Fujita reports an anemometer recording which shows winds of 67 m/sec (150 mph) at the edge of a damage path of a tornado generated an hour later by the same storm. The conclusion therefore is that the actual circulation of the twin tornado was much greater than the value $(4.92 \times 10^3 \ \mathrm{m^2/sec})$ calculated from its revolution rate by assuming that the vortices moved with the fluid. Apparently, the revolution rate was retarded with respect to the fluid by at least a factor of 1/2.

The possibility of local wind shear causing this retardation has been considered. A continuous source of wind shear is the tornado cyclone in which tornado J-2 was embedded. This wind shear can be estimated from the paths of the family of tornadoes generated by the tornado cyclone, as presented in the maps of reference 4. The wind shear estimated in this way is found to be too low to affect the revolution rate of the twin tornado J-2 significantly.

# REFERENCES

1. Fujita, Tetsuya: Formation and Steering Mechanisms of Tornado Cyclones and Associated Hook Echoes. Mon. Weather Rev., vol. 93, no. 2, Feb. 1965, pp. 67-78.

2. Browning, Keith A.; and Fujita, T.: A Family Outbreak of Severe Local Storms — A Comprehensive Study of the Storms in Oklahoma on 26 May 1963, Part I. AFCRL-65-695(1), U.S. Air Force, Sept. 1965.

3. Fujita, Tetsuya: Estimated Wind Speeds of the Palm Sunday Tornadoes. SMRP Res. Pap. No. 53 (ESSA Grant No. E-86-67-(G)), Univ. of Chicago, Apr. 1967.

4. Fujita, Tetsuya: Aerial Survey of the Palm Sunday Tornadoes of April 11, 1965. SMRP Res. Pap. No. 49 (Grant WBG-41(NSSL)), Univ. of Chicago, Jan. 1966.

5. Lamb, Horace: Hydrodynamics. Sixth ed., Dover Publ., Inc., 1945.

6. Serrin, J.: Mathematical Principles of Classical Fluid Mechanics. Encycl. Phys., vol. VIII, pt. 1, Fluid Dynamics I, S. Flügge, ed., Springer-Verlag (Berlin), 1959, pp. 125-263.

7. Sommerfeld, Arnold: Mechanics of Deformable Bodies. Academic Press, Inc., c.1950.

8. Tsien, H. S.: The Equations of Gas Dynamics, Fundamentals of Gas Dynamics, Howard W. Emmons, ed., Princeton Univ. Press, 1958, pp. 3-63.

9. Godske, C. L.; Bergeron, T.; Bjerknes, J.; and Bundgaard, R. C.: Dynamic Meteorology and Weather Forecasting. Amer. Meteorol. Soc. and Carnegie Inst. of Washington, 1957.

10. Howarth, L.: The Equations of Flow in Gases. Modern Developments in Fluid Dynamics — High Speed Flow, Vol. 1, L. Howarth, ed., Clarendon Press (Oxford), 1953, pp. 34-70.

11. Goldman, Joseph L.: The Role of the Kutta-Joukowski Force in Cloud Systems With Circulation. Tech. Note 48-NSSL-27, Weather Bur., U.S. Dep. Com., June 1966, pp. 21-34.

12. Brooks, Edward M.: Tornadoes and Related Phenomena. Compendium of Meteorology, Thomas F. Malone, ed., Amer. Meteorol. Soc., 1951, pp. 673-680.

13. Namias, Jerome; and Clapp, Philip F.: Observational Studies of General Circulation Patterns. Compendium of Meteorology, Thomas F. Malone, ed., Amer. Meteorol. Soc., 1951, pp. 551-567.

14. Abdullah, Abdul Jabbar: Some Aspects of the Dynamics of Tornadoes. Mon. Weather Rev., vol. 83, no. 4, Apr. 1955, pp. 83-94.

15. Lewis, William; and Perkins, Porter J.: Recorded Pressure Distribution in the Outer Portion of a Tornado Vortex. Mon. Weather Rev., vol. 81, no. 12, Dec. 1953, pp. 379-385.

16. Vonnegut, B.; and Weyer, James R.: Luminous Phenomena in Nocturnal Tornadoes. Science, vol. 153, no. 3741, Sept. 9, 1966, pp. 1213-1220.

17. Rossow, Vernon J.: On the Origin of Circulation for Tornado Formation. Twelfth Conference on Radar Meteorology, Amer. Meteorol. Soc., 1967, pp. 183-189.

18. Busemann, Adolf: Relations Between Aerodynamics and Magnetohydrodynamics. Proceedings of the NASA-University Conference on the Science and Technology of Space Exploration, Vol. 2, NASA SP-11, 1962, pp. 305-312.

19. Busemann, Adolf: On the Kármán Vortex Street in Magnetofluid-Dynamics. Aerospace Scientific Symposium of Distinguished Lecturers honoring Von Kármán on 80th Anniversary, Inst. Aerosp. Sci., c.1962, pp. 87-110.

20. Vonnegut, Bernard: Electrical Theory of Tornadoes. J. of Geophys. Res., vol. 65, no. 1, Jan. 1960, pp. 203-212.

21. Silberg, P. A.: Dehydration and Burning Produced by the Tornado. J. Atmos. Sci., vol. 23, no. 2, Mar. 1966, pp. 202-205.

22. Colgate, Stirling A.: Tornadoes: Mechanism and Control. Science, vol. 157, no. 3795, Sept. 22, 1967, pp. 1431-1434.

23. Brook, Marx: Electric Currents Accompanying Tornado Activity. Science, vol. 157, no. 3795, Sept. 22, 1967, pp. 1434-1436.

24. Rossow, Vernon J.: Observations of Waterspouts and Their Parent Clouds. NASA TN D-5854, 1970.

## TABLE I.- PARAMETERS FOR TWIN TORNADO J-2

### OBTAINED FROM FIGURE 4

| Location | Center-to-center separation in ground plane, $R_c$ | | Tilt angle with respect to vertical, $\chi$, deg | Azimuth angle, $\psi_A$, deg | $\Gamma_B/\Gamma_A$ |
|---|---|---|---|---|---|
| | ft | m | | | |
| 3 | 390 | 118.9 | 31 | 96.9 | 0.6 |
| 4 | 431.8 | 131.6 | 29 | 134.1 | 1.00 |
| 5 | 478.2 | 145.7 | 29 | 151.4 | 1.35 |
| 6 | 482.6 | 147.1 | 29 | 237.0 | 2.75 |

## TABLE II.- MEAN VALUES FOR PARAMETERS OF TABLE I AND

### MEAN OBSERVED REVOLUTION RATES FOR TORNADO J-2

| Interval between locations | Mean separation, $\langle R_c \rangle$ | | Mean tilt angle, $\langle \chi \rangle$, deg | Mean azimuth angle, $\langle \psi_A \rangle$, deg | Mean revolution rate (observed), $\langle \dot{\psi}_A \rangle$, rad/sec | $\langle \Gamma_B/\Gamma_A \rangle$ | $\langle D \rangle$ (eq. (70c)) |
|---|---|---|---|---|---|---|---|
| | ft | m | | | | | |
| 3-4 (13 sec) | 410.9 | 125.2 | 30 | 115.5 | 0.05 | 0.8 | 1.1 |
| 4-5 (8 sec) | 455.0 | 138.7 | 29 | 142.8 | .038 | 1.17 | .973 |
| 5-6 (31 sec) | 480.4 | 146.4 | 29 | 194.2 | .048 | 2.05 | .891 |

"The aeronautical and space activities of the United States shall be
conducted so as to contribute . . . to the expansion of human knowl-
edge of phenomena in the atmosphere and space. The Administration
shall provide for the widest practicable and appropriate dissemination
of information concerning its activities and the results thereof."

— NATIONAL AERONAUTICS AND SPACE ACT OF 1958

# NASA SCIENTIFIC AND TECHNICAL PUBLICATIONS

**TECHNICAL REPORTS:** Scientific and
technical information considered important,
complete, and a lasting contribution to existing
knowledge.

**TECHNICAL NOTES:** Information less broad
in scope but nevertheless of importance as a
contribution to existing knowledge.

**TECHNICAL MEMORANDUMS:**
Information receiving limited distribution
because of preliminary data, security classifica-
tion, or other reasons.

**CONTRACTOR REPORTS:** Scientific and
technical information generated under a NASA
contract or grant and considered an important
contribution to existing knowledge.

**TECHNICAL TRANSLATIONS:** Information
published in a foreign language considered
to merit NASA distribution in English.

**SPECIAL PUBLICATIONS:** Information
derived from or of value to NASA activities.
Publications include conference proceedings,
monographs, data compilations, handbooks,
sourcebooks, and special bibliographies.

**TECHNOLOGY UTILIZATION
PUBLICATIONS:** Information on technology
used by NASA that may be of particular
interest in commercial and other non-aerospace
applications. Publications include Tech Briefs,
Technology Utilization Reports and Notes,
and Technology Surveys.

*Details on the availability of these publications may be obtained from:*

## SCIENTIFIC AND TECHNICAL INFORMATION DIVISION

# NATIONAL AERONAUTICS AND SPACE ADMINISTRATION
### Washington, D.C. 20546